12-15-2018

Optimal placement of distributed energy storage systems in distribution networks using artificial bee colony algorithm

Choton K. Das
Edith Cowan University

Octavian Bass
Edith Cowan University

Ganesh Kothapalli
Edith Cowan University

Thair S. Mahmoud

Daryoush Habibi

10.1016/j.apenergy.2018.07.100

Optimal Placement of Distributed Energy Storage Systems in Distribution Networks using Artificial Bee Colony Algorithm

Choton K. Das[a,*], Octavian Bass[a], Ganesh Kothapalli[a], Thair S. Mahmoud[b], Daryoush Habibi[a]

[a] *School of Engineering, Edith Cowan University (ECU), 270 Joondalup Drive, Joondalup, Perth, WA 6027, Australia*

[b] *Australian Maritime College, University of Tasmania (UTAS), Launceston, Tasmania 7250, Australia*

Abstract

The deployment of utility-scale energy storage systems (ESSs) can be a significant avenue for improving the performance of distribution networks. An optimally placed ESS can reduce power losses and line loading, mitigate peak network demand, improve voltage profile, and in some cases contribute to the network fault level diagnosis. This paper proposes a strategy for optimal placement of distributed ESSs in distribution networks to minimize voltage deviation, line loading, and power losses. The optimal placement of distributed ESSs is investigated in a medium voltage IEEE-33 bus distribution system, which is influenced by a high penetration of renewable (solar and wind) distributed generation, for two scenarios: (1) with a uniform ESS size and (2) with non-uniform ESS sizes. System models for the proposed implementations are developed, analyzed, and tested using DIgSILENT PowerFactory. The artificial bee colony optimization approach is employed to optimize the objective function parameters through a Python script automating simulation events in PowerFactory. The optimization results, obtained from the artificial bee colony approach, are also compared with the use of a particle swarm optimization algorithm. The simulation results suggest that the proposed ESS placement approach can successfully achieve the objectives of voltage profile improvement, line loading minimization, and power loss reduction, and thereby significantly improve distribution network performance.

Keywords: Energy storage systems, energy storage system allocation, voltage profile improvement, line loading reduction, power loss minimization, particle swarm optimization.

Nomenclature

Δt Time interval

*Corresponding author

Email addresses: cdas@our.ecu.edu.au (Choton K. Das), o.bass@ecu.edu.au (Octavian Bass), g.kothapalli@ecu.edu.au (Ganesh Kothapalli), thair.mahmoud@utas.edu.au (Thair S. Mahmoud), d.habibi@ecu.edu.au (Daryoush Habibi)

Accepted in *Applied Energy*

η_c ESS charging efficiency

η_d ESS discharging efficiency

γ_{ESS} Weighting factor for ESS cost

Γ_{LL} Line loading cost rate

γ_{LL} Weighting factor for line loading cost

Γ_{loss} Power loss cost rate

γ_{PL} Weighting factor for power losses cost

Γ_{VD} Voltage deviation cost rate

γ_{VD} Weighting factor for voltage deviation cost

ζ_i Load weighting factor of ith bus

$\mathcal{J}(C_{Fi})$ Objective function which is a function of cost

aP, bP, & cP Real power coefficients for phase a, b, & c

aQ, bQ, & cQ Reactive power coefficients for phase a, b, & c

C_{LL}^{l} Cost for line loading

C_{PL}^{l} Cost for power losses

C_{VD}^{n} Cost for voltage deviation

CS Colony size in ABC optimization

$E_{ESS-max}$ Maximum ESS energy

$E_{ESS-min}$ Minimum ESS energy

E_{ESS} ESS energy

E_{ESS}^{t+1} ESS energy at time $t+1$

E_{ESS}^{t} ESS energy at time t

I_{ij-max} Current limit of line ij

I_{ij}^{t} Current magnitude through line ij

It_{max} Maximum number of iterations in ABC optimization

K Total number of active ESSs on the network

L_{trial} Trial limit for improving a food source in ABC optimization

$lb1$ Lower boundary of decision variable S_{ESS}^{i}

$lb2$ Lower boundary of decision variable λ_{ESS}^{i}

M Total number of lines

N Total number of buses

N_D Number of decision variables in ABC optimization

N_{FS} Number of food sources in ABC optimization

$P_{ESS-max}$ Maximum ESS power

$P_{ESS-min}$ Minimum ESS power

P_{ESS} ESS power

$P^d_{i\to k}$ Real power delivered from i to a neighbouring bus k

P^c_i Real power consumed at bus i

P^g_i Real power generated at bus i

$P^d_{j\to i}$ Power delivered to i from a neighbouring bus j

P^l_{L-base} Real power loss for base case (without ESS)

P^l_{L-ESS} Real power loss with optimal ESS placement

P_{LT} Total real power loss

$P_L(i,j)$ Real power loss of a line connecting two buses, i and j

$P^t_{ESS,c}$ ESS charging power at time t

$P^t_{ESS,d}$ ESS discharging power at time t

P^t_{ESS} ESS power at time t

$PLRI_P$ Real power loss reduction index with optimal ESS placement

$PLRI_Q$ Reactive power loss reduction index with optimal ESS placement

$PLRI_T$ Total power loss reduction index with optimal ESS placement

$Q^d_{i\to k}$ Reactive power delivered from i to a neighbouring bus k

Q^c_i Reactive power consumed at bus i

Q^g_i Reactive power generated at bus i

$Q^d_{j\to i}$ Reactive power delivered to i from a neighbour bus j

Q^l_{L-base} Reactive power loss for base case (without ESS)

Q^l_{L-ESS} Reactive power loss with optimal ESS placement

Q_{LT} Total reactive power loss

$Q_L(i,j)$ Reactive power loss of a line connecting two buses, i and j

$R_L(i,j)$ Resistance of a line connecting two buses, i and j

$S_{ESS-max}$ Maximum ESS size

$S_{ESS-min}$ Mimimum ESS size

S_{Li} Load at bus i in p.u.

S_{wind} Total capacity (kVA) of wind DG

SL^{l-t} Loading of line l

SL^{l}_{base} Loading of line l without ESS placement

SL^{l}_{ESS} Loading of line l after ESS placement

SL^{l}_{max} Maximum loading of line l

SL^{l}_{rated} Rated ampacity of line l

SOC^{k}_{ESS} State of charge of kth ESS

$ub1$ Upper boundary of decision variable S^{i}_{ESS}

$ub2$ Upper boundary of decision variable λ^{i}_{ESS}

UUC Ultrabattery unit cost

V_{bi} Bus voltage of ith bus in per unit (p.u.)

V^{t}_{bi} voltage magnitude at different times t in a day

V^{+}_{i} Positive sequence voltage

V^{-}_{i} Negative sequence voltage

V_{max} Upper voltage limit

V_{min} Lower voltage limit

V_{rated} Rated voltage of the system in p.u.

V_{ref} Reference bus voltage in p.u.

V_{target} Target voltage of the system

VUF_{max} Maximum VUF

$X_L(i,j)$ Reactance of a line connecting two buses, i and j

1. Introduction

Present power systems face a period of rapid change driven by various interrelated issues, e.g., demand management [1], greenhouse gas (GHG) reduction targets [2], integration of renewables [3, 4], power congestion [5], power quality requirements [6, 7], and network expansion [8] and reliability [6, 7]. For distribution networks, an energy storage system (ESS) converts electrical energy from a power network, via an external interface, into a form that can be stored and converted back to electrical energy when needed [9]. Depending on the

demand or cost benefits, the ESS can store energy to produce and discharge electricity [10]. Consequently, ESSs are increasingly being embedded in distribution networks to offer technical, economic, and environmental advantages. These include mitigation of voltage deviation [11, 12], facilitation of renewable energy source (RES) integration [13–15], distributed generation planning [16] and RES energy time-shifting [17], load shifting [18–21], load levelling [22] and peak shaving [23], power quality improvement [5, 11, 24, 25], frequency regulation [5, 26], network expansion [27, 28] and overall cost reduction [29, 30], operating reserves [5, 31], GHG reduction [32–34], profit maximization [5, 35], and network reliability [36].

Unfortunately, misplacement or misuse of ESSs in distribution networks can adversely affect network performance [37], voltage and frequency regulation, power quality, reliability, and load controllability. Appropriate ESS placement can facilitate an optimal ESS operation for voltage and power quality improvement [5, 12, 24, 25], peak demand mitigation [12], relief of distribution congestion [5, 25], power flow adjustment [5], power loss reduction [12, 25], network reliability [36], overall network cost reduction [36, 38], RESs integration [27, 39, 40], and system effectiveness [36, 41]. As the use of large-scale ESSs in distribution networks involves substantial investment, placing ESSs optimally on the basis of performance expectations is challenging and has been addressed in several studies [5, 11, 12, 24, 25, 27, 29, 30, 36, 38, 39, 41–51].

Asset management of distribution networks is an essential task of network service providers to ensure safe and secure operation of the networks. However, this can be an expensive task that also might result in a high network cost and thereby can significantly affect electricity prices. This cost could include network reinforcement for thermal and voltage stability. Therefore, the motivation of this work is to provide low cost solutions to distribution network operators for a better asset management practice.

A comprehensive review, regarding ESS placement to mitigate the issues of distribution networks, is presented in [9]. An optimal allocation and sizing of ESSs, for an IEEE-30 wind power distribution system, is accomplished in [24], while focusing on power system cost minimization and voltage profile improvement. The authors employ a hybrid multi-objective particle swarm optimization (PSO) incorporating a non-dominated sorting genetic algorithm (NSGA-II), a probabilistic load flow technique, and a five-point estimation method (5PEM).

In [42], a multi-objective ESS allocation is performed for both transmission and distribution networks. A detailed analysis, termed as sensitive analysis, is accomplished on the transmission side using complex-valued neural networks, time domain power flow, and economic dispatch to locate the ESSs. On distribution side, the optimal ESS size is estimated to address load curve smoothing and peak load shaving. [41] proposes optimal distributed ESS planning (specifying locations and sizes) in soft open points-based distribution networks embedding the reactive power capability of distributed generators (DGs) and the network reconfiguration through a mixed-integer second order cone programming (MISOCP) approach. [29] formulates an optimal ESS placement problem embedding network reconfiguration in an RES-integrated distribution network to minimize overall system costs, while employing a mixed-integer linear programming (MILP) approach.

Optimal ESS location and size are determined in [43] for load management, minimization of net present value (NPV), and total cost while maximizing distribution system benefits.

A genetic algorithm (GA) combined with a linear programming solver, a sequential Monte Carlo simulation (MCS), and MATLAB optimization toolbox are used for different aspects of the investigations. The same approaches are used in [36] and [30] to establish optimal ESS allocations in different situations. [36] accomplishes optimal ESS allocation, targeting minimization of interruption cost and annual cost, and improvement of distribution system reliability. On the other hand, distribution network benefits are maximized in [30] by reducing the cost of ESS installation, maintenance, interruptions, system upgrades, and energy losses.

An optimal allocation of distributed community ESSs in distribution networks is proposed in [27] to gain the benefits from peaking PV generation, energy arbitrage, energy loss reduction, emission reduction, network upgrade deferral, and Var support. [38] proposes a network-aware strategy for the planning and control of ESSs in an RES-penetrated distribution network to minimize investment and operational costs. [44] analyzes the impact of ESS location and configuration on power losses, voltage profiles, and ESS utilization within a feeder of low voltage (LV) distribution networks.

The mitigation of voltage deviations and improvement of supply quality, elimination of load curtailment and line congestions, and minimization of distribution network costs and electricity costs are achieved through the optimal placement and sizing of ESSs, while using AC-optimal power flow (AC-OPF) and MISOCP approaches in [11]. In [45], a fuzzy PSO (FPSO) approach is employed to mitigate the risk to distribution companies by optimizing ESS allocation, while maximizing energy transaction profits and reducing operational costs.

In [5], a MILP model is proposed to maximize the net profit of distributed ESSs while achieving distribution system congestion management, energy price arbitrage and energy reserve, and a frequency regulation service via active and reactive power controls. In [39], the ESS allocation is able to minimize the voltage fluctuation problems (due to PV integrations in LV networks) by applying a GA-based strategy hybridized with simulated annealing, while [46] employs a GA-based bi-level optimization approach to mitigate the same problem. Again in [25], an alternating direction approach to multipliers is employed for allocation of distributed ESSs to provide voltage support and to minimize both network losses and the cost of energy in relation to external grid and congestion management.

In [47], optimal ESS placement and sizing is accomplished and validated through mathematical modeling and the OPF approach. A game-theoretic multi-agent approach is proposed in [48] for optimal ESS allocation to mitigate the risk of energy transaction mechanisms for energy agents. In [49], optimal ESS allocation in LV distribution networks is accomplished through multi-period OPF and clustering and sensitivity analysis approaches to prevent under- and over-voltages and to minimize total network costs (in regard to ESS and network losses).

A framework for optimal ESS placement in a wind-penetrated deregulated power system is developed in [50] to maximize the utilization of wind power and minimize the hourly social cost. Market-based probabilistic OPF, GA, and an energy arbitrage model are applied to optimize, evaluate, and analyze the system model. An auto-regression moving average modeling technique, for optimal ESS placement in a wind-penetrated distribution grid, is proposed to minimize the annual electricity cost without considering peak shaving and reliability enhancement in [51]. [12] achieves optimally distributed ESS allocation and

operation in order to improve load and generation hosting ability, while using a cost-based multi-objective optimization strategy through MATLAB. As a result, power loss and peak demand are reduced, with better voltage regulation.

Although various distribution network issues are addressed in the above literature, very few studies [12] focus on line loading minimization, power loss reduction, and voltage profile improvement. However, the operational costs of distribution networks are largely dependent on these parameters which can be minimized through optimal distributed ESS placement. For a large distribution network, distributed ESS placement provides more opportunities for problem mitigation and greater flexibility than centralized placement [24, 50]. For instance, this approach helps to fix the voltage deviation in buses promptly, which is done generally with on-load tap changers, capacitors and voltage regulators [52]. In some research [30, 36, 43, 48] (as discussed above) the ESS types, such as lead-acid, vanadium redox (VR), sodium sulfur (NaS), compressed air energy storage (CAES), and Li-ion, are specified. Other research [11, 24, 25, 27, 39, 41] does not specify ESS types. However, in [12, 42, 44, 46] ESS name is mentioned as battery ESS (BESS) rather than specifying the ESS technology, e.g., lead-acid, Li-ion or other.

The determination of optimal ESS locations in a distribution network involves one or more optimization problems depending on the benefits targeted. Various optimization and modeling techniques are employed for the optimal placement of ESSs in the above literature [5, 11, 12, 24, 25, 27, 29, 30, 36, 38, 39, 41–45, 47–51]. The research described in this paper introduces artificial bee colony (ABC) meta-heuristic optimization for optimal ESS placement. Being simple and robust, the ABC algorithm is capable of solving even complex combinatorial and multi-dimensional optimization problems [53, 54]. The likelihood of finding an optimum solution is enhanced by the algorithm's triple search capability, which is based on the search stages of three groups of bees [55, 56]. The robustness and efficiency of the ABC algorithm in solving global optimization problems (both constrained and unconstrained) is demonstrated in various comparative studies that compare the ABC algorithm to other well-known modern heuristic algorithms such as GA, DE, and PSO [55, 56].

In this paper, a comprehensive investigation is carried out for optimal ESS placement in an IEEE-33 bus distribution network, in a distributed manner. DIgSILENT PowerFactory provides useful solutions for distribution network problems such as system design, modeling and optimization capabilities, grid interaction skills in a multi-user environment, and data handling [57]. As a result, it is used as the main tool for system modeling and analysis. Python programming language is used to control the system models developed in PowerFactory and to facilitate the ABC optimization. Furthermore, a new form of lead-acid battery, the Ultrabattery, is selected as the ESS technology and is used in this research.

The main contributions of this paper are summarized as follows:

- The optimal placement of ESSs is investigated focusing on line loading reduction, real and reactive power loss minimization, voltage profile improvement, and ultimately cost minimization. All of the parameters, incorporated in the objective function, are related to costs of distribution network reinforcement for thermal and voltage stability, and lower asset management. These parameters have not been widely considered together for optimal ESS placement by other studies such as [24, 25, 44, 49]. Furthermore, some important constraints which are rarely used by earlier works such as voltage

unbalance factor (VUF) and line loading constraints are imposed in this study.

- The overall investigation for optimal ESS placement is conducted in two different categories: (1) with a uniform ESS size, and (2) with non-uniform ESS sizes. These type of investigations have not been conducted by earlier works such as [11, 12, 25, 44, 45, 48, 50, 51]. The results from these investigations are analyzed and compared. Although the ABC approach is used for these investigations, PSO algorithm is also applied to justify the optimality of results obtained from ABC optimization technique.

- The performance indices are evaluated and a cost comparison for various case studies is presented. These performance indices assist to follow-up the performance improvement after ESS allocation in a distribution network, which are not evaluated by related studies in the literature.

The remainder of this paper is organized as follows: the overall system modeling including ESS selection, and ESS and distribution network modeling are presented in Section II. The problem is formulated in Section III and the optimization and proposed approach are discussed in Section IV. Section V discusses the testing and performance measurement. The results are presented and discussed in Section VI. The paper concludes with Section VII.

2. System modeling

2.1. ESS selection and modeling

The appropriate selection of grid-scale ESSs depends on various factors such as required system performance, system capacity, type of application, and ESS cost and reliability [9, 58, 59]. Various ESS options for distribution networks, to be explored in terms of technical characteristics and application benefits, are discussed in [9, 60, 61]. A recent ESS, namely Ultrabattery (also known as an advanced lead-acid battery), is frequently being incorporated in grid-scale applications in the U.S. and Australia, due to its improved performance and lower cost in comparison with other electrochemical ESSs (e.g., lead-acid) [62, 63]. The lead sulfate accumulation problem of lead-acid batteries is reduced in the Ultrabattery by incorporating carbons and forming a supercapacitor. Given the above considerations, Ultrabatteries are chosen as ESSs in this research.

Although the Ultrabattery is chosen as the ESS technology in this research, the ESS model is considered as generic and can be applied to other ESS technologies. The ESS model should be subjected to the following conditions:

- If state of charge (SOC^k_{ESS}) = 1, the ESS is fully charged and if $SOC^k_{ESS} = 0$, the ESS is fully discharged.

- The ESS should be able to control the active power in both ways and the SOC^k_{ESS} is subject to following constraint [64]:

$$0.2 \leqslant SOC^k_{ESS} \leqslant 0.9 \tag{1}$$

- A priority for the active and reactive power (P and Q) is needed to satisfy the apparent rated power, $S_{app} = \sqrt{P^2 + Q^2}$.

Additionally, the proposed ESS should fulfill boundary conditions from (1) to (6) in time t (indexed $1, ..., NT$) [12, 65]. The charging and discharging rates are determined by (1) and (2), respectively, by applying the generator convention (the charging power is positive i.e. $P^t_{ESS,c} > 0$ and the discharging power is negative i.e. $P^t_{ESS,d} < 0$) [66]. The energy storing process and charging power of the ESS are restricted by (3) and (4) respectively. Moreover, the limitations of released energy from the ESS and power discharged by the ESS are demonstrated by (5) and (6) respectively.

$$P^t_{ESS,c} = max\left\{ P_{ESS-min}, \frac{(E^t_{ESS} - S_{ESS-max})}{\eta_c \cdot \Delta t} \right\} \tag{2}$$

$$P^t_{ESS,d} = min\left\{ P_{ESS-max}, \frac{(E^t_{ESS} - S_{ESS-min})\,\eta_d}{\Delta t} \right\} \tag{3}$$

Charging mode:

$$E^{t+1}_{ESS} = min\left\{ \left(E^t_{ESS} - \Delta t\ P^t_{ESS,c}\ \eta_c\right),\ S_{ESS-max} \right\} \tag{4}$$

$$P^t_{ESS,c} \leqslant P^t_{ESS} \leqslant P^t_{ESS,d} \tag{5}$$

Discharging mode:

$$E^{t+1}_{ESS} = max\left\{ \left(E^t_{ESS} - \Delta t\ \ \frac{P^t_{ESS,d}}{\eta_d}\right),\ S_{ESS-min} \right\} \tag{6}$$

$$P^t_{ESS,c} \leqslant P^t_{ESS} \leqslant P^t_{ESS,d} \tag{7}$$

2.2. Distribution network model

The modeling of the proposed medium voltage (MV) distribution network is accomplished in DIgSILENT PowerFactory. The single line diagram of the proposed system (for the case of optimal ESS placement with a uniform ESS size) is depicted in Fig. 1, where the IEEE-33 bus radial distribution system is used to model the overall system. The buses and lines are denoted by the letters B and L, respectively. The loads, solar DGs, and wind DGs are modeled using built-in templates of PowerFactory and configured according to system data found in [12, 67]. The ESS model, described in Section II(A), is placed on the network in a distributed manner. The chosen base MVA and substation voltage are 10 MVA and 12.66 kV, respectively, and the power factor is considered as unity. Among 37 lines, L33 to L37 are represented as tie lines [67]. In this model, a high renewable DG penetration scenario is created by installing seven solar DGs and two wind DGs. The three solar DGs of 400kVA capacity each (PV1, PV2, and PV3) are allocated to B05, B21, and B31, while the other four of 500kVA capacity (PV4, PV5, PV6, and PV7) are installed on B08, B12, B28, and B33, respectively. All other system data are taken from [67]. The wind DGs of 1MW

capacity (WDG1 and WDG2) are placed on B18 and B24 [12]. B01 is defined as the feeder of the whole system and peak active and reactive power input to feeder are 3.715 MW and 2.3 MVar, respectively.

The power flow equations of the model are given in [24, 68], which are solved using the Newton-Raphson method.

3. Problem formulation

3.1. Objective function

The objective function (8) is formulated to solve the optimal distributed ESS placement problem using (9) to (15) [12, 69]. The cost function includes the costs regarding network reinforcement for thermal and voltage stability, and lower asset management of distribution networks. Overall cost minimization is achieved by minimizing the sum of cost factors, e.g., performance costs (C^n_{VD}, C^l_{PL}, and C^l_{LL}) and ESS cost (C^{UT}_{ESS}), while satisfying the necessary constraints. The cost factors are weighted equally with γ_{VD}=γ_{PL}=γ_{LL}=γ_{ESS}=1.

$$\mathcal{J}(C_{Fi}) = minimize \left\{ \underbrace{\left(\gamma_{VD}\cdot C^n_{VD} + \gamma_{PL}\cdot C^l_{PL} + \gamma_{LL}\cdot C^l_{LL}\right)}_{C_{performance}} + \left(\gamma_{ESS}\cdot\ C^{UT}_{ESS}\right) \right\} \tag{8}$$

where,

$$C^n_{VD} = \left(\sum_{n=1}^{N} |V_{target} - V_{bi}(s^i_{ESS}, \lambda^i_{ESS})| \right) \cdot \Gamma_{VD} \tag{9}$$

$$C^l_{PL} = \left(\sqrt{\{P_{LT}(s^i_{ESS}, \lambda^i_{ESS})\}^2 + \{Q_{LT}(s^i_{ESS}, \lambda^i_{ESS})\}^2} \right) \cdot \Gamma_{loss} \tag{10}$$

$$P_{LT}(S^i_{ESS}, \lambda^i_{ESS}) = \sum_{l=1}^{M} P_L(i,j) \ = \sum_{l=1}^{M} \left(R_L(i,j) \ \cdot \frac{P_i^2 + Q_i^2}{|\ \{\ V_{bi}(s^i_{ESS}, \lambda^i_{ESS})\}^2|} \right) \tag{11}$$

$$Q_{LT}(S^i_{ESS}, \lambda^i_{ESS}) = \sum_{l=1}^{M} Q_L(i,j) \ = \sum_{l=1}^{M} \left(X_L(i,j) \ \cdot \frac{P_i^2 + Q_i^2}{|\ \{\ V_{bi}(s^i_{ESS}, \lambda^i_{ESS})\}^2|} \right) \tag{12}$$

$$C^l_{LL} = \sum_{l=1}^{M} \left(\%\ LL_{ESS}(s^i_{ESS}, \lambda^i_{ESS}) \right) \cdot \Gamma_{LL} \tag{13}$$

$$\%\ LL_{ESS}(s^i_{ESS}, \lambda^i_{ESS}) = \left(\frac{SL^l_{ESS}}{SL^l_{rated}} \right) \times 100 \tag{14}$$

The total ESS unit cost is calculated as follows [70]:.

$$C^{UT}_{ESS} = \sum_{i=1}^{K} S^i_{ESS} \cdot UUC \tag{15}$$

In the above equations, $\Gamma_{VD} = 0.142$ \$ p.u. [12], $\Gamma_{loss} = 0.265$ \$/kWh [71], $\Gamma_{LL} = 0.503$ \$ p.u. [71], and $V_{target} = 1$ p.u.. In addition, the UUC for commercial and industrial energy management applications is considered as 460 \$/kWh [72].

3.2. Objective function constraints

The objective function of (8) is subject to (16) to (27) together with ESS modeling equations as given in (1) to (7):

$$P_i^g + \sum_{j \in J+} \left(P_{j \to i}^d\right) = P_i^c + \sum_{k \in J-} \left(P_{i \to k}^d\right) \tag{16}$$

$$Q_i^g + \sum_{j \in J+} \left(Q_{j \to i}^d\right) = Q_i^c + \sum_{k \in J-} \left(Q_{i \to k}^d\right) \tag{17}$$

$$V_{min} < |V_{bi}^t| < V_{max} \tag{18}$$

$$VUF < VUF_{max} \tag{19}$$

$$VUF = \sum_{i=1}^{n} \frac{V_i^+}{V_i^-} \times 100 \tag{20}$$

$$I_{ij}^t < I_{ij-max} \tag{21}$$

$$SL^{l-t} < SL_{max}^l \tag{22}$$

$$\lambda_{ESS}^i = \begin{cases} 0, & \textit{if the ESS is active} \\ 1, & \textit{otherwise} \end{cases} \tag{23}$$

$$S_{ESS}^i = \begin{cases} Assign, & if\ \lambda_{ESS}^i = 0 \\ 0, & if\ \lambda_{ESS}^i = 1 \end{cases} \tag{24}$$

$$P_{ESS-min} < P_{ESS} < P_{ESS-max} \tag{25}$$

$$P_{ESS,c}^t \leq P_{ESS}^t \leq P_{ESS,d}^t \tag{26}$$

$$E_{ESS-min} < E_{ESS} < E_{ESS-max} \tag{27}$$

where,

- (16) and (17) denote that the real and reactive power delivered to and from a bus i must be balanced [73].
- (18) indicates the voltage magnitude constraint of each node. (19) denotes a constraint for voltage unbalanced factor (VUF) as defined in (20) to avoid any voltage imbalance due to voltage fluctuations. The $VUF = 0$ indicates perfectly balanced voltages in a distribution system and generally $VUF_{max} = 1$ [12].
- (22) ensures that the line loading of a line l should not exceed the maximum limit SL_{max}^l to ensure the cable's thermal stability. By referring to industry practices of planning, the operation of distribution networks should not exceed 80% loading on the substation exit cables [74]. Hence, an 80% maximum loading target of a line l is imposed in the algorithm. This also ensures that there is sufficient spare capacity among feeders to back each other during outages.

- (23) and (24) represent the ESS allocation constraints.
- (25) to (27) ensures that the power or energy of ESSs should not exceed their boundary limits during charging and discharging [12]. In addition, (1) to (7) ensure the ESS operation within the SOC limit.

4. Optimization and proposed approach

4.1. ABC optimization approach

In this paper, the ABC algorithm is employed for optimizing the grid-connected ESS allocation problem. The ABC algorithm is a relatively new bio-inspired swarm intelligence approach and one of the recent metaheuristic search techniques proposed by Karaboga in 2005 [75]. This algorithm is proposed to simulate the intelligent foraging behaviour of honey bees. This has the advantage of using fewer control parameters [54, 76]. The colony consists of three types of bees in the ABC algorithm: employed bees, onlooker bees, and scout bees. Specifically, its robust searching ability encompasses the exploitation and exploration of the search space [75]. This exploitation process is performed during the employed and onlooker bee phase, while during the scout bee phase the exploration process is accomplished. The overall ABC optimization process is illustrated by the flow chart given in Fig. 2.

There is only one employed bee for every food source. By using the following expression, each employed bee moves from one old location x_{ij} to a new candidate location v_{ij}:

$$v_{ij} = x_{ij} + \phi_{ij}\left(x_{ij} - x_{kj}\right) \tag{28}$$

In (28), $k \in 1, 2, .., SN$ and $j \in 1, 2, .., D$ are randomly chosen and k has to be different from i, where, SN = the number of food sources, D = problem dimension, and ϕ_{ij} = uniform random number in the range [-1, 1]. If the new location value v_{ij} is better than x_{ij}, then x_{ij} is updated and replaced with v_{ij}, otherwise x_{ij} is kept unchanged. Depending on the probability value, the onlooker bee selects a food source by using a roulette wheel selection method and this new position is then determined by (29), where, ω_i = weight coefficient of employed bee information.

$$v_{ij} = x_{ij} + \omega_i\phi_{ij}\left(x_{ij} - x_{kj}\right) \tag{29}$$

The food source probability (p_i) and the fitness values of the food sources of employed bees (fit) are calculated according to (30) and (31), respectively, where, $f(x_i)$ denotes the number of objective function values to be optimized.

$$p_i = \frac{fit_i}{\sum_{j=1}^{SN} fit_j} \tag{30}$$

$$fit_i = \begin{cases} \frac{1}{1+f(x_i)}, & f(x_i) \geq 0 \\ 1 + |f(x_i)|, & f(x_i) < 0 \end{cases} \tag{31}$$

4.2. Proposed approach

The proposed methodology for resolving the optimal distributed ESS placement problem is represented in Fig. 3. The optimization parameters and variables are summarized in Table 1. After modeling, configuring, and placing all required components in the distribution system of Fig. 1, all the essential system data are entered in the corresponding components and the ABC parameters are initialized. The total active and reactive powers for the feeder (P_{TF} & Q_{TF}) are entered for feeder load scaling and the operational capacity of solar DGs (S_{pv-op}) is considered as 85% of rated capacity (S_{pv-max}) [77]. Subsequently, the loads, solar, and wind DGs are characterized by applying time-variant characteristics [12]. The feeder loads are scaled by creating voltage dependency. Then the problem is formulated to minimize the total of C^n_{VD}, C^l_{PL}, C^l_{LL}, and C^{UT}_{ESS}.

The investigations are accomplished in two phases- (1) Investigation type-I: with a uniform ESS size and (2) Investigation type-II: with non-uniform ESS sizes. The ESS size (S^i_{ESS}) and positions (λ^i_{ESS}) are generated randomly and applied to the system. The S^i_{ESS} is generated in such a way that the maximum number of ESSs with lower capacity (within the range 0.1 MVA to 2 MVA) can be distributed in the network. The initial values are selected randomly by relying on the nominated range of sizes to be tested on the network. The ESS size nomination is subject to $lb1$, $ub1$, $lb2$, $ub2$, transformer size, DC and AC bus size, inverter specifications, and ESS string size. Finally, the ABC optimization process finds the optimal values of S^i_{ESS} and λ^i_{ESS} by satisfying the objective function constraints.

In this paper, the sizing approach considers a unity power factor applied on the dispatch of ESSs. This is based on common industry practices that distribution network operators will not rely on the distributed generators to solve the network voltage problem, but rather rely on the substation automatic voltage controllers and distributed capacitors to control the MVars. Hence, the ESS size and locations are determined based on using the multi-functionality of ESSs in providing the MW required to minimize line losses and loading, and support the voltage controllers on the network. This approach maintains the voltage at the desired levels proposed by operation requirements.

5. Testing and performance measurement

This section describes the application of necessary factors of load model and RES generation, feeder load scaling, and voltage dependency in the proposed distribution network model. Furthermore, it states the essential indices to measure the performance improvement of the system.

5.1. Assignment of factors and dependency

Feeder load scaling and voltage dependency: Considering the scaling factor, the load is calculated according to (32) and (33) [78]. The load scaling of a distribution feeder, consisting of loads Load$i$, is presented in Fig. 4. The Ψ_{scale} is adjusted so that the total real and reactive powers are calculated as (34) and (35), respectively [78].

$$P = \Psi_{scale} \cdot \ P_0 \tag{32}$$

$$Q = \Psi_{scale} \cdot \ Q_0 \tag{33}$$

$$\begin{aligned} P = \Psi_{scale} \cdot \ P1_0 + \ \Psi_{scale} \cdot \ P2_0 + \ \Psi_{scale} \cdot \ P3_0 + \\ \ldots\ldots + \ \Psi_{scale} \cdot \ Pn_0 \end{aligned} \tag{34}$$

$$\begin{aligned} Q = \Psi_{scale} \cdot \ Q1_0 + \ \Psi_{scale} \cdot \ Q2_0 + \ \Psi_{scale} \cdot \ Q3_0 + \\ \ldots\ldots + \ \Psi_{scale} \cdot \ Qn_0 \end{aligned} \tag{35}$$

Taking into account the voltage dependency of loads, (32) and (33) are converted to (36) and (37), respectively, where, $(1 - aP - bP) = cP$ and $(1 - aQ - bQ) = cQ$.

$$\begin{aligned} P = \Psi_{scale} \cdot \ P_0 \ \Bigg[aP \cdot \left(\frac{V_{bi}}{V_{ref}}\right)^{e_{aP}} + \ bP \cdot \left(\frac{V_{bi}}{V_{ref}}\right)^{e_{bP}} \\ + (1 \ -aP-bP) \cdot \left(\frac{V_{bi}}{V_{ref}}\right)^{e_{cP}} \Bigg] \end{aligned} \tag{36}$$

$$\begin{aligned} Q = \Psi_{scale} \cdot \ Q_0 \ \Bigg[aQ \cdot \left(\frac{V_{bi}}{V_{ref}}\right)^{e_{aQ}} + \ bQ \cdot \left(\frac{V_{bi}}{V_{ref}}\right)^{e_{bQ}} \\ + (1 \ -aQ-bQ) \cdot \left(\frac{V_{bi}}{V_{ref}}\right)^{e_{cQ}} \Bigg] \end{aligned} \tag{37}$$

Load and generation scaling factors: The loads of the distribution network follow the IEEE-RTS model as depicted in Fig. 5 and the load coefficients are set to $aP = aQ = 0.4$, $bP = bQ = 0.3$, and $cP = cQ = 0.3$ [12]. The exponents are assigned to $e_{aP} = e_{aQ} = 0$, $e_{bP} = e_{bQ} = 1$, and $e_{cP} = e_{cQ} = 2$ to model the load behaviour as constant power, constant current, and constant impedance, respectively, for corresponding load coefficients [78]. The generation outputs of solar PV and wind DGs are scaled according to the curves of Fig. 5 [12].

5.2. System performance indices

Voltage deviation and profile improvement indices: As the minimization of voltage fluctuations is crucial for the operation of the power systems, the permissible voltage deviation limit is considered as $\pm 5\%$ in this research. The voltage deviation index (VDI) of (38), expressed as a percentage, represents the system voltage deviation [79].

$$\%\ VDI = \sum_{i=1}^{N} \left(\frac{|V_{rated} - V_{bi}|}{V_{rated}} \right) \times 100 \tag{38}$$

The voltage profile of ith bus of the system can be defined as (39) [80]. The V_{max} and V_{min} for ith bus are determined by the voltage violation limit ($\pm 5\%$).

$$VP_i = V_{bi}\ S_{Li}\ \zeta_i \tag{39}$$

The incorporation of a load weighting factor (ζ_i) has considerable impact on the voltage profile improvement index ($VPII$), which allows the possibility of a low load bus with

voltage sensitive loads. Generally, these factors are assigned based on the criticality or importance of the load at each bus. It is assumed that all the loads of the proposed system have equal importance. For the overall network, the total of all factors ζ_i is defined as (40).

$$\sum_{i=1}^{N} \zeta_i = 1 \tag{40}$$

Hence, the overall voltage profile of the system can be expressed as (41).

$$VP = \sum_{i=1}^{N} VP_i \tag{41}$$

The $VPII$, a measure of the improved voltage profile of the proposed distribution system, can be defined as (42) [80].

$$VPII = \frac{VP_{w-ESS}}{VP_{wo-ESS}} \tag{42}$$

Power loss reduction indices: The real, reactive, and total power loss reduction indices ($PLRI_P$, $PLRI_Q$, and $PLRI_T$) are defined by (43), (44), and (45), respectively [79, 80].

$$PLRI_P = \frac{\sum_{l=1}^{M} P^l_{L-ESS}}{\sum_{l=1}^{M} P^l_{L-base}} \tag{43}$$

$$PLRI_Q = \frac{\sum_{l=1}^{M} Q^l_{L-ESS}}{\sum_{l=1}^{M} Q^l_{L-base}} \tag{44}$$

$$PLRI_T = \frac{\sum_{l=1}^{M} \sqrt{\left(P^l_{L-ESS}\right)^2 + \left(Q^l_{L-ESS}\right)^2}}{\sum_{l=1}^{M} \sqrt{\left(P^l_{L-base}\right)^2 + \left(Q^l_{L-base}\right)^2}} \tag{45}$$

Line loading index: The line loading index (LLI) refers to the loading level or demand of the distribution system lines. Minimizing line loading through optimally placed ESSs may be an effective way of deferring distribution investment. In other words, the distribution network peak demand can be reduced by minimizing the LLI. This may also minimize the investment costs for distribution network expansion. This is necessary in order to increase the system's tolerance of load growth. In this research, the percent line loading ($\%LL$) for a specific line, total percent line loading ($\%LLT$) (before and after ESS placement), and the overall LLI are formulated by (14) and (46) to (49).

$$\%\ LL_{base} = \left(\frac{SL^l_{base}}{SL^l_{rated}}\right) \times 100 \tag{46}$$

$$\%\ LLT_{w-ESS} = \sum_{l=1}^{M} \%\ LL_{ESS} \tag{47}$$

$$\%\ LLT_{wo-ESS} = \sum_{l=1}^{M} \%\ LL_{base} \tag{48}$$

$$LLI = \frac{\%\ LLT_{w-ESS}}{\%\ LLT_{wo-ESS}} \tag{49}$$

6. Results and discussion

After optimization and testing, the system performance is analyzed in three different case studies. Optimal ESS locations are determined while minimizing the cost function at peak load condition. This section describes the impact of optimal distributed ESS allocation in the proposed distribution system. The ESSs only inject P (MW) to the network and the power factor is unity. The system results are categorized for three cases: base case (without ESS), ESS placement while considering a uniform ESS size, and non-uniform ESS sizes. These are presented in Table 2. Case 2 and Case 3 are investigated in two different subcategories based on the weighting factor selection of $\mathcal{J}(C_{Fi})$ as given in Table 2. Although the factors in (8) are equally weighted (Case 2(I) and Case 3(I)), γ_{VD} is changed to 100 along with γ_{PL}=γ_{LL}=γ_{ESS}=1 in Case 2(II) and Case 3(II) to give more importance to C^n_{VD} than other parameters. This comparison is presented targeting better realization of the optimization results. It is assumed that the ESS power rating (MVA) is constant over one hour.

6.1. Case study 1- Base case without ESSs

The results of parameter $\%VDI$, $\%LLT$, P_T, and Q_T for base case analysis (without the placement of ESSs), tabulated in Table 2 represent the reference values which are targeted to be optimized. Although the V_{bi} is within maximum and minimum voltage limits, the voltage profile needs improvement. Similar results are observed for other parameter values.

6.2. Case study 2- ESS allocation for a uniform ESS size

Case 2, optimal ESS placement for a uniform S^i_{ESS}, is divided in two different categories with two different combinations of S^i_{ESS} and λ^i_{ESS}. The S^i_{ESS} and λ^i_{ESS} can be identified in Table 2 by the ESS MVA and ESS number, respectively: e.g., ESS9 = 0.724 represents that the ESS of size 0.724 MVA is connected to bus9. It is noticeable that all Case 2(I) parameters ($\%VDI$, $\%LLT$, P_T, and Q_T) are minimized compared to Case 1. Although Case 2(II) minimizes the C^n_{VD} − i.e. improves the voltage profile ($\%VDI = 32.238$) − the $\%LLT$, P_T, and Q_T exceed the corresponding values for Case 1. Furthermore, the total ESS size is 23.689 MWh, which represents a higher distribution system investment cost and hence is unacceptable. For Case 2(I), the required number of optimally placed ESSs in the network is 8 with $S^i_{ESS} = 0.724$ MVA, while it is 12 with $S^i_{ESS} = 1.974$ MVA for Case2(II). Hence, considering the optimal performance as well as costs and a negotiation of $\%VDI$, Case 2(I) is the required optimal solution with minimum ESS size (5.793 MWh) for Investigation type-I.

6.3. Case study 3- ESS allocation for non-uniform ESS sizes

The impact of optimal distributed ESS allocation with non-uniform S^i_{ESS} is analyzed and the results are listed in Table 2. Case 3(I) shows the optimization results with minimum $\mathcal{J}(C_{Fi})$, while Case 3(II) represents the outcome for minimum C^n_{VD}. A very noticeable point is that all the parameters ($\%VDI$, $\%LLT$, P_T, and Q_T) are further reduced compared to Case 2(I). However, for Case 3(I), the required number of optimally placed ESSs is 11 and

total ESS size is 7.195 MWh, which represents an increment in cost over Case 2(I). The total ESS size is further increased to 18.425 MWh while minimizing C_{VD}^{n} (41.520) in Case 3(II). For this case, the other parameters ($\%LLT$, P_T, and Q_T) are higher compared to Case 2(I) and Case 3(I).

6.4. Overall result comparison and analysis

Comparison of voltage profiles: The voltage profiles for various cases are depicted in Fig. 6. The feeder voltage profiles (p.u. voltage vs km) after ESS placement, i.e. for Case 2 and Case 3 of Table 2, are illustrated in Fig. 7 to Fig. 10, where various sections in terms of feeder length are marked with different colors. In the distribution network model, all the lines have the same length (1km). At some buses, the p.u. voltages for the particular feeder length are illustrated. According to Fig. 7 and Fig. 6, the bus voltages vary within 1 p.u. to 0.967 p.u. for Case 2(I), while the lowest voltage value (0.967 p.u.) is observed at B30. B18 and B33 have about the same voltage of 0.973 p.u, while the similar voltage value of around 0.972 p.u. is obtained at B16 and B31. Case 3(I) has a better feeder voltage profile compared to Case 2(I) as presented in Fig. 9 and Fig. 6. The voltages at various bus during Case 3(I) are improved, e.g., at B16 (Case 3(I)=0.976 p.u., Case 2(I)=0.972 p.u.), at B31 & B32 (Case 3(I)=0.975 p.u., Case 2(I)=0.972 p.u.), and at B33 (Case 3(I)=0.976 p.u., Case 2(I)=0.973 p.u.). The Case 2(II) provides the best voltage profile compared to other cases as per Fig. 6 to Fig. 10. During this case, most of the bus voltages vary around the target voltage 1 p.u. as presented in Fig. 8, while the lowest voltage of 0.97 p.u. is observed at B24. The voltages at some buses, e.g., B09, B15, and B14 are above the V_{target}. On the other hand, Case 3(II) also provides an improver voltage profile than Case 2(I) and Case 3(I). However, there are higher voltage drops at some buses compared to Case 2(II) such as at B6 (Case 3(II)=0.978 p.u., Case 2(II)=0.981 p.u.), B8 (Case 3(II)=0.980 p.u., Case 2(II)=0.987 p.u.), B12 (Case 3(II)=0.985 p.u., Case 2(II)=0.997 p.u.), B20 (Case 3(II)=0.986 p.u., Case 2(II)=0.992 p.u.), B21(Case 3(II)=0.985 p.u., Case 2(II)=0.993 p.u.), and B27 (Case 3(II)=0.981 p.u., Case 2(II)=0.985 p.u.). There are also improvements on voltages at some buses in Case 3(II) compared to Case 2(II), for instance, at B17 (Case 3(II)=1.002 p.u., Case 2(II)=0.997 p.u.), B18 (Case 3(II)=1.001 p.u., Case 2(II)=0.999 p.u.), B25 (Case 3(II)=0.983 p.u., Case 2(II)=0.976 p.u.), and B33 (Case 3(II)=1.001 p.u., Case 2(II)=0.998 p.u.).

It may also be noted that the voltage drop in the feeder section numbered L02-L22-L23-L24-L37-L29-L30 is higher for Case 2(I), Case 2(II), and Case 3(I) compared to other sections of Fig. 1, and there is an improvement in this characteristic for Case 3(II). In contrast, the voltage drop in the feeder section numbered L18-L19-L20-L21-L35 is lower than other sections for all cases except Case 2(I) where the voltage drop in L20 is slightly higher compared to other cases. Case 2(II) provides an improved feeder voltage profile compared to Case 3(II) and most of the bus voltages are very close to 1 p.u. for Case 2(II) except B07, B23, B24, B25, B29, and B30. The voltages of these buses are further improved (except B07) in Case 3(II) while having little voltage deviation in other buses compared to Case 2(II). Hence, it is evident that Case 2(II) and Case 3(II) have better voltage profiles among the options, while Case 2(I) and Case 3(I) provide good voltage profiles.

Comparison of line loading and losses: The percent line loadings of various cases are presented in Fig. 11. This suggests that the loading of lines for each case is under the maximum limit. For Case 2(II) and Case 3(II) the line loadings are higher, while Case 2(II) provides the worst loading in lines especially in L8, L22, L26, L28, L30, L35, and L37. Case 2(I) and Case 3(I) have good line loading among the options, while the best characteristics are provided by Case 3(I). Although the maximum loading limit of a line is 80%, L1 has maximum loading of 40.801% for all cases. L2 has around 28% loading for Case 1, Case 3(I), and Case 3(II), while it has a lower (27.633%) and a higher (31.908%) loading value for Case 2(I) and Case 2(II), respectively. All other lines for most of the cases are more lightly loaded (below 15%) except L30 and L37. For Case 2(II), the L30 and L37 are loaded around 27%, while L37 in Case 3(II) is loaded about 22%. It can be noted from the line loading characteristics that the overall feeder has sufficient spare capacity to tackle the worst situation during outage condition by sharing the loads with others.

The real, reactive, and total power losses of lines for various cases, with respect to individual line numbers, are compared in Fig. 12, Fig. 13, and Fig. 14, respectively. According to Fig. 12, L2 has a real power loss of 0.0347 MW, 0.0271 MW, and 0.0269 MW for Case 2(II), Case 3(I), and Case 3(II), respectively. Case 2(II) and 3(II) provide higher real power losses (compared to other cases) in L30 which are 0.0513 MW and 0.0387 MW, respectively. The L8 has a real power loss of 0.0424MW for Case 2(II) which is higher than other cases. It is also noticeable for all cases that there is no real power loss in tie lines (L33 to L37) as illustrated in Fig. 12. As referred to Fig. 13, higher reactive power loss is delivered during Case 2(II) compared to other cases, specifically in L2, L8, L30, L35, and L37. In L2, Case 2(I), Case 3(I), and Case 3(II) have the similar amount of reactive power loss which is 0.0133 MVar, 0.0138 MVar, and 0.0137 MVar, respectively, while it is a bit higher (0.0177 MVar) for Case 2(II). In L8, Case 2(II) and Case 3(II) have a higher reactive power loss of 0.0305 MVar and 0.0088 MVar, respectively. Case 3(II) gives the highest reactive power loss of 0.0190 MVar and 0.0112 MVar in L16 and L24, respectively. In L30, Case 2(II) has the highest reactive power loss of 0.0507 MVar compared to all other lines. Remarkably, all cases provide reactive power loss to the tie lines (L33 to L37), while higher losses are added by Case 2(II) and Case 3(II) compared to others. Overall, according to the illustrations of Fig. 12, Fig. 13, and Fig. 14, the losses are higher for Case 2(II) and Case 3(II) and lower for Case 2(I) and Case 3(I). Again, the worst case for total line loss is Case 2(II), while having larger amount of loss in L2, L8, L30, L35, and L37 compared to other cases.

Statistical analysis of ABC approach with PSO algorithm: The well-known PSO algorithm [81] is employed to verify the ESS allocation results of Case 2(I) and Case3(I) obtained from the ABC approach. Cognitive and social components of PSO are both set to 1.8, while the inertia weight is selected as 0.6 as recommended in [55]. The ABC settings are listed in Table 1. The ABC optimization and the PSO are executed for 30 times considering a maximum iteration value of 1000, a population size of 50, and γ_{VD}=γ_{PL}=γ_{LL}=γ_{ESS}=1 in (8). From the list of obtained results, the best, worst, and mean objective function solutions are compared in Table 3 for the two investigation types. Furthermore, the standard deviations for ABC and PSO approaches (σ_{ABC} and σ_{PSO}) of objective function values are evaluated. The lesser standard deviation value represents smaller deviation among solutions

of 30 times optimization runs. Although both algorithms provides very close solutions in terms of objective function costs, it is evident from Table 3 that the more optimal solutions are obtained from the ABC for both investigation types. For instance, the ABC best solution for investigation type-I signifies the improvement in performance such as $\%VDI = 75.753$, $\%LLT = 241.128$, $P_T = 0.0905$ MW, and total ESS size (5.793 MWh) except little deviation in Q_T (0.0683 MVar) compared to PSO best solution (i.e. $VDI = 76.894$, $\%LLT = 241.633$, $P_T = 0.0917$ MW, $Q_T = 0.0677$ MVar, and total ESS size=6.007 MWh). Hence, it is obvious from the statistical analysis of Table 3 that the proposed ABC-based approach is successful in achieving required optimal solutions for both investigation types.

The configuration of the used computer for conducting the optimization is: Intel(R) Xeon 3.5 GHz processor, 16 GB RAM, 64-bit windows 10. Fig. 15 represents the convergence test of the ABC and PSO algorithms for two investigation types. The convergence results and computation time are summarized in Table 4. This suggests that the ABC-based approach converges after 208 and 347 iterations for investigation type-I and investigation type-II, respectively. On the contrary, PSO algorithm converges after 191 and 332 iterations for investigation type-I and investigation type-II, respectively. In other words, the PSO algorithm converges faster than the ABC approach. In real time, ABC and PSO algorithms require around 325 s and 440 s, respectively, to locate the ESSs under investigation type-I. For investigation type-II, the ABC and PSO approaches take about 503 s and 665 s, respectively, to place the ESSs on the network.

Overall performance and ESS cost comparison: The performance indices of the proposed system are evaluated and presented in Table 5. Generally, the system has a good voltage profile for $VPII > 1$. For instance, the $VPII = 2.114$ for Case 2(II) represents that Case 2(II) has the best voltage profile among the options. On the other hand, the higher values of $PLRI_P$, $PLRI_Q$, $PLRI_T$, and LLI denote higher real power loss, reactive power loss, total line loss, and line loading, respectively. For example, Case 3(I) has the $PLRI_T = 0.802$ and the $LLI = 0.890$ which are lower than those of Case 2(I) ($PLRI_T = 0.816$ & $LLI = 0.894$). This implies that Case 3(I) has achieved improved performance in regard to total line loss and line loading compared to Case 2(I).

Fig. 16 presents the overall comparison of the system performance indices and total ESS unit cost (as the total ESS unit cost is the highest cost component of the system, which is defined in (15)). It is apparent from the characteristics that case 2(I) is relatively cost efficient and is the optimal solution for distributed ESS allocation with a uniform size, while Case 3(I) is the optimal choice for ESS allocation with non-uniform sizes.

7. Conclusions

This paper has presented an effective strategy for the optimal placement of distributed ESSs in distribution networks using the ABC meta-heuristic optimization technique. The key problems of voltage deviation, line loading, and power losses in distribution networks are addressed and mitigated to improve system performance. The PSO algorithm is also applied to verify the system results obtained from the ABC approach. The related performance indices are evaluated and overall system results are analyzed quantitatively. Based on the investigations and analysis presented in this paper, the following conclusions can be made

in regard to optimal ESS placement:

- The optimal placement of multiple ESSs, in a distributed manner, offers good flexibility and performance improvement in a distribution network with large renewable DG penetration.
- Both approaches − optimal distributed ESS placement with a uniform size and non-uniform sizes − are suitable for solving distribution network issues as addressed in this paper. However, ESS placement with a uniform size technique can be implemented more flexibly, while the approach with non-uniform ESS sizes is more adjustable with regard to performance improvement.
- As the optimal ESS placement largely depends on performance improvement targets, a tradeoff should be made in terms of performance indices, installation sites, and costs. For instance, considering optimal performance as well as implementation costs, and a tradeoff with voltage profile, line loading, and losses, Case 2(I) presented in Section VI is the optimal solution.

Overall, considering the above findings, the proposed approach for optimal placement of distributed ESSs is highly suitable for an MV or large-scale distribution system and can be used in real distribution network planning and asset management applications. Future work can apply intelligent control techniques that consider the online communication among the placed ESSs. Optimal operation of ESSs considering RES uncertainty, comprehensive ESS sizing, ESS placement by injecting both P and Q on the dispatch of ESSs, and overall power quality improvement after ESS placement can also be investigated.

Acknowledgment

This research is supported by Edith Cowan University (ECU) and an Australian Government Research Training Program (RTP) scholarship. We gratefully acknowledge the technical support and assistance of Mr Wayne Ong of DIgSILENT PACIFIC, Melbourne, Australia.

Appendices

A. System data

The system data used for the IEEE 33 distribution network test system is presented in Table 6 [67].

Table 1: Summary of ABC optimization parameters and variables

Type	**Parameters/variables**	**Description/settings**
Input parameters	V_{rated},$R_L(i,j)$, $X_L(i,j)$, P, Q, P_{TF}, Q_{TF}, S_{wind}, S_{PV-max}, S_{PV-op}, and $S_{ESS-max}$	Required for the network model.
Output parameters	C^n_{VD}, C^l_{PL}, C^l_{LL}, and C^{UT}_{ESS}	Required for the objective function.
Decision variables	S^i_{ESS}	Determines the ESS size in MVA with unity power factor, i.e. the ESSs inject only P (MW) to the network ($Q = 0$).
	λ^i_{ESS}	This determines the ESS position in the network.
ABC parameters	N_D, CS, N_{FS}, L_{trial}, and It_{max}	Settings: $N_D = 2$, $CS = 100$, $N_{FS} = CS/2$ =population size, $L_{trial} = 60$, and $It_{max} = 1000$.
ABC bounds	For S^i_{ESS}: $lb1$ and $ub1$	Settings: $lb1 = 0.1$ MVA and $ub1 = 2$ MVA.
	For λ^i_{ESS}: $lb2$ and $ub2$	Settings: $lb2 = 0$ and $ub2 = 1$.

Table 2: System results after a quantitative analysis

Case Details	**ESS Apparent Power (MVA) & Locations**	**%VDI**	**%LLT**	**P_T (MW)**	**Q_T (MVar)**	**Total ESS Size (MWh)**
Case 1	**Without ESS allocation**					
Base case	No ESS	89.73	269.81	0.11	0.09	-
Case 2	**Distributed ESS allocation for a uniform ESS size**					
(I). Min $\mathcal{J}(C_{Fi})$ with γ_{VD}=γ_{PL}=γ_{LL}=γ_{ESS}=1	ESS9, ESS14, ESS25, ESS28, ESS29, ESS30, ESS31, ESS32, ESS MVA=0.724	75.753	241.128	0.0905	0.0683	5.793
(II). Min $\mathcal{J}(C_{Fi})$ with γ_{VD}=100 & γ_{PL}=γ_{LL}=γ_{ESS}=1	ESS9, ESS11, ESS14, ESS15, ESS25, ESS27, ESS28, ESS29, ESS30, ESS31, ESS32, ESS33, ESS MVA=1.974	32.238	440.955	0.2491	0.2691	23.689
Case 3	**Distributed ESS allocation for non-uniform ESS sizes**					
(I). Min $\mathcal{J}(C_{Fi})$ with γ_{VD}=γ_{PL}=γ_{LL}=γ_{ESS}=1	ESS8=0.335, ESS10=0.378, ESS13=0.383, ESS16=0.823, ESS17=0.1, ESS20=0.128, ESS22=0.1, ESS25=2, ESS30=1.442, ESS31=0.725, ESS32=0.781	72.162	240.039	0.0894	0.0666	7.195
(II). Min $\mathcal{J}(C_{Fi})$ with γ_{VD}=100 & γ_{PL}=γ_{LL}=γ_{ESS}=1	ESS9=0.28, ESS11=1.13, ESS13=0.454, ESS14=1.42, ESS15=0.735, ESS17=2, ESS25=2, ESS26=0.11, ESS27=0.711, ESS28=1.427, ESS29=2, ESS30=2, ESS31=1.873, ESS32=1.603, ESS33=0.682	41.520	388.220	0.1830	0.2100	18.425

Table 3: Statistical analysis of ABC and PSO approaches for 30 runs

Optimization statistics	**ESS apparent power (MVA) & locations**	**%VDI**	**%LLT**	P_T **(MW)**	Q_T **(MVar)**	**Total ESS size (MWh)**	**Objective function value ($)**
Investigation type-I: Distributed ESS allocation for a uniform ESS size							
ABC best	ESS9, ESS14, ESS25, ESS28, ESS29, ESS30, ESS31, ESS32, ESS MVA=0.724	75.753	241.128	0.0905	0.0683	5.793	26,65,008.853
ABC worst	ESS7, ESS13, ESS15, ESS25, ESS28, ESS29, ESS30, ESS31, ESS32, ESS MVA= 0.667	77.534	242.162	0.0909	0.0684	6.000	27,60,040.417
ABC mean	ESS7, ESS9, ESS15, ESS25, ESS29, ESS30, ESS31, ESS32, ESS MVA=0.747	76.967	241.642	0.0918	0.0677	5.972	27,47,375.519
σ_{ABC}							16374.188
PSO best	ESS7, ESS9, ESS15, ESS25, ESS29, ESS30, ESS31, ESS32, ESS MVA=0.751	76.894	241.633	0.0917	0.0677	6.007	27,63,254.781
PSO worst	ESS7, ESS9, ESS15, ESS25, ESS28, ESS29, ESS30, ESS31, ESS32, ESS MVA= 0.693	77.836	242.296	0.0918	0.0685	6.235	28,67,990.169
PSO mean	ESS7, ESS13, ESS15, ESS25, ESS28, ESS29, ESS30, ESS31, ESS32, ESS MVA= 0.673	77.426	242.168	0.0908	0.0685	6.053	27,84,573.115
σ_{PSO}							19574.237
Investigation type-II: Distributed ESS allocation for non-uniform ESS sizes							
ABC best	ESS8=0.335, ESS10=0.378, ESS13=0.383, ESS16=0.823, ESS17=0.1, ESS20=0.128, ESS22=0.1, ESS25=2, ESS30=1.442, ESS31=0.725, ESS32=0.781	72.162	240.039	0.0894	0.0666	7.195	33,09,852.689
ABC worst	ESS5=0.1, ESS9=0.556, ESS11=0.1, ESS15=0.836, ESS17=0.1, ESS22=0.1, ESS24=0.1, ESS25=1.479, ESS26=0.164, ESS28=0.1, ESS30=2.0, ESS31=1.589, ESS33=0.121	72.623	243.322	0.0889	0.0678	7.345	33,78,653.069
ABC mean	ESS8=0.162, ESS10=0.181, ESS13=0.237, ESS15=0.512, ESS21=0.1, ESS24=0.101, ESS25=1.736, ESS26=0.310, ESS28=0.159, ESS30=2.0, ESS31=0.492, ESS32=1.226	73.954	241.143	0.0867	0.0679	7.216	33,19,390.463
σ_{ABC}							12939.034
PSO best	ESS7=0.379, ESS10=0.403, ESS14=0.1, ESS15=1.878, ESS25=1.772, ESS27=0.1, ESS30=2.0, ESS31=0.465, ESS33=0.1	74.494	240.923	0.0853	0.0671	7.197	33,10,730.059
PSO worst	ESS6=0.193, ESS8=0.1, ESS9=0.1, ESS10=0.470, ESS12=0.383, ESS15=0.429, ESS16=0.149, ESS21=0.1, ESS22=0.1, ESS25=2.0, ESS29=0.273, ESS30=1.112, ESS31=2.0	72.969	243.505	0.0909	0.0696	7.409	34,08,087.049
PSO mean	ESS6=0.1, ESS10=0.334, ESS11=0.1, ESS14=0.1, ESS15=0.921, ESS16=0.1, ESS17=0.147, ESS25=1.447, ESS28=0.1, ESS29=0.449, ESS30=2.0, ESS31=1.462	72.053	242.983	0.0862	0.0675	7.260	33,39,593.907
σ_{PSO}							19310.970

Table 4: Convergence and computation time of ABC and PSO algorithms

Investigation type	**ABC convergence**	**ABC computation time (s)**	**PSO convergence**	**PSO computation time (s)**
I	After 208 iterations	325	After 191 iterations	440
II	After 347 iterations	503	After 332 iterations	665

Table 5: Performance indices for various cases of Table 2

Case Details	$\boldsymbol{VPII}$	$\boldsymbol{PLRI_P}$	$\boldsymbol{PLRI_Q}$	$\boldsymbol{PLRI_T}$	$\boldsymbol{LLI}$
Case 1	-	-	-	-	-
Case 2(I)	1.037	0.829	0.802	0.816	0.894
Case 2(II)	2.114	2.281	3.158	2.755	1.634
Case 3(I)	1.064	0.819	0.781	0.802	0.890
Case 3(II)	1.823	1.675	2.408	2.059	1.439

Table 6: Used data for 33-bus test system [67]

Line Number	**Sending Bus**	**Receiving Bus**	**Resistance (Ω)**	**Reactance (Ω)**	**Load at Receiving End Bus**	
					Real Power (kW)	**Reactive Power (kVar)**
L01	B01 (Main SS)	B02	0.0922	0.0477	100	60
L02	B02	B03	0.4930	0.2511	90	40
L03	B03	B04	0.3660	0.1864	120	80
L04	B04	B05	0.3811	0.1941	60	30
L05	B05	B06	0.8190	0.7070	60	20
L06	B06	B07	0.1872	0.6188	200	100
L07	B07	B08	1.7114	1.2351	200	100
L08	B08	B09	1.0300	0.7400	60	20
L09	B09	B10	1.0400	0.7400	60	20
L10	B10	B11	0.1966	0.0650	45	30
L11	B11	B12	0.3744	0.1238	60	35
L12	B12	B13	1.4680	1.1550	60	35
L13	B13	B14	0.5416	0.7129	120	80
L14	B14	B15	0.5910	0.5260	60	10
L15	B15	B16	0.7463	0.5450	60	20
L16	B16	B17	1.2890	1.7210	90	40
L17	B17	B18	0.7320	0.5740	90	40
L18	B2	B19	0.1640	0.1565	90	40
L19	B19	B20	1.5042	1.3554	90	40
L20	B20	B21	0.4095	0.4784	90	40
L21	B21	B22	0.7089	0.9373	90	40
L22	B3	B23	0.4512	0.3083	90	50
L23	B23	B24	0.8980	0.7091	420	200
L24	B24	B25	0.8960	0.7011	420	200
L25	B6	B26	0.2030	0.1034	60	25
L26	B26	B27	0.2842	0.1447	60	25
L27	B27	B28	1.0590	0.9337	60	20
L28	B28	B29	0.8042	0.7006	120	70
L29	B29	B30	0.5075	0.2585	200	600
L30	B30	B31	0.9744	0.9630	150	70
L31	B31	B32	0.3105	0.3619	210	100
L32	B32	B33	0.3410	0.5302	60	40
L33⋆⋆	B21	B8	0.0000	2.0000		
L34⋆⋆	B9	B15	0.0000	2.0000		
L35⋆⋆	B12	B22	0.0000	2.0000		
L36⋆⋆	B18	B33	0.0000	0.5000		
L37⋆⋆	B25	B29	0.0000	0.5000		
⋆⋆= Tie Lines, Substation Voltage = 12.66 kV						

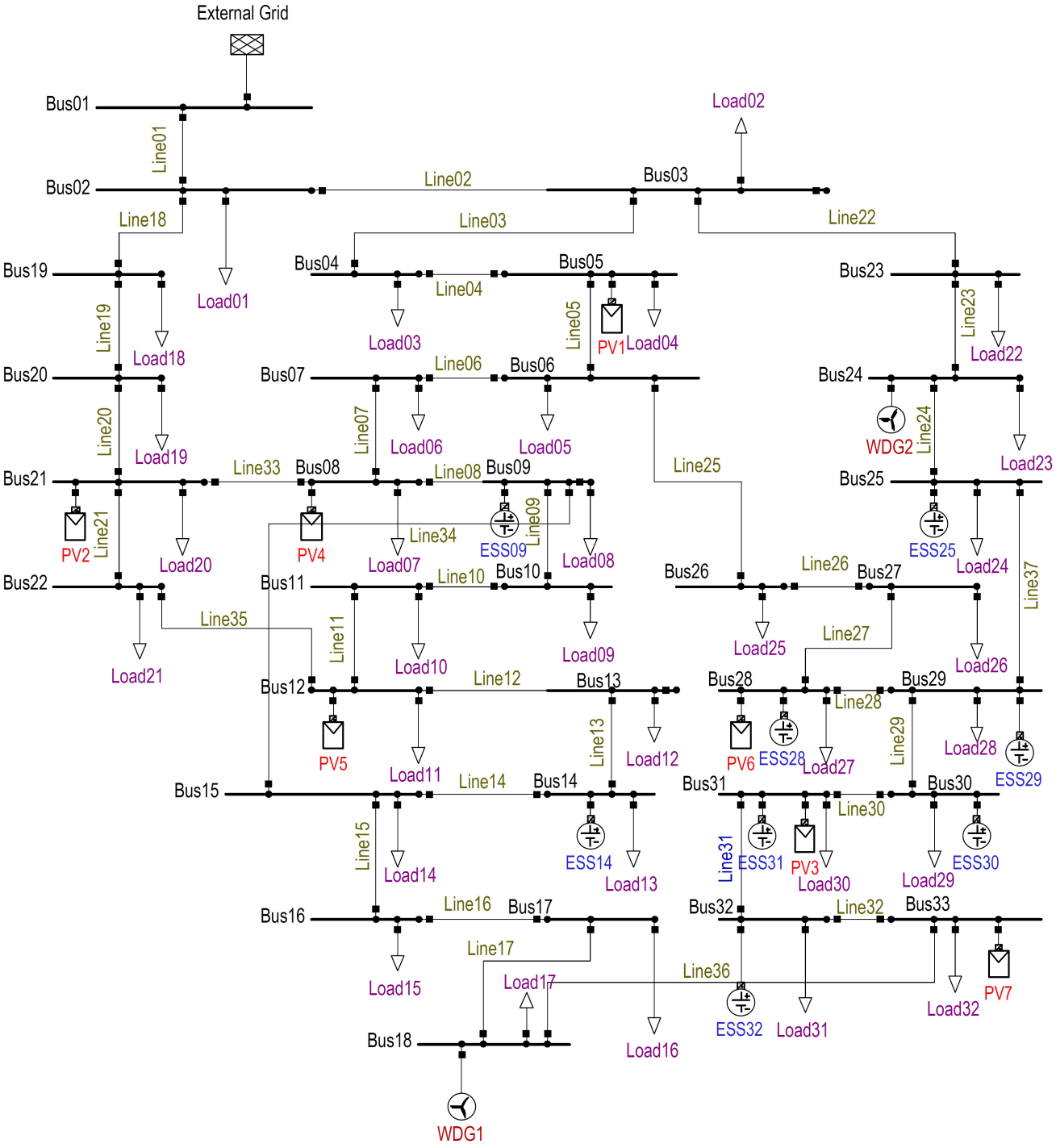

Figure 1: Single-line diagram of the proposed distribution network model (ESS placement for Case 2(I)).

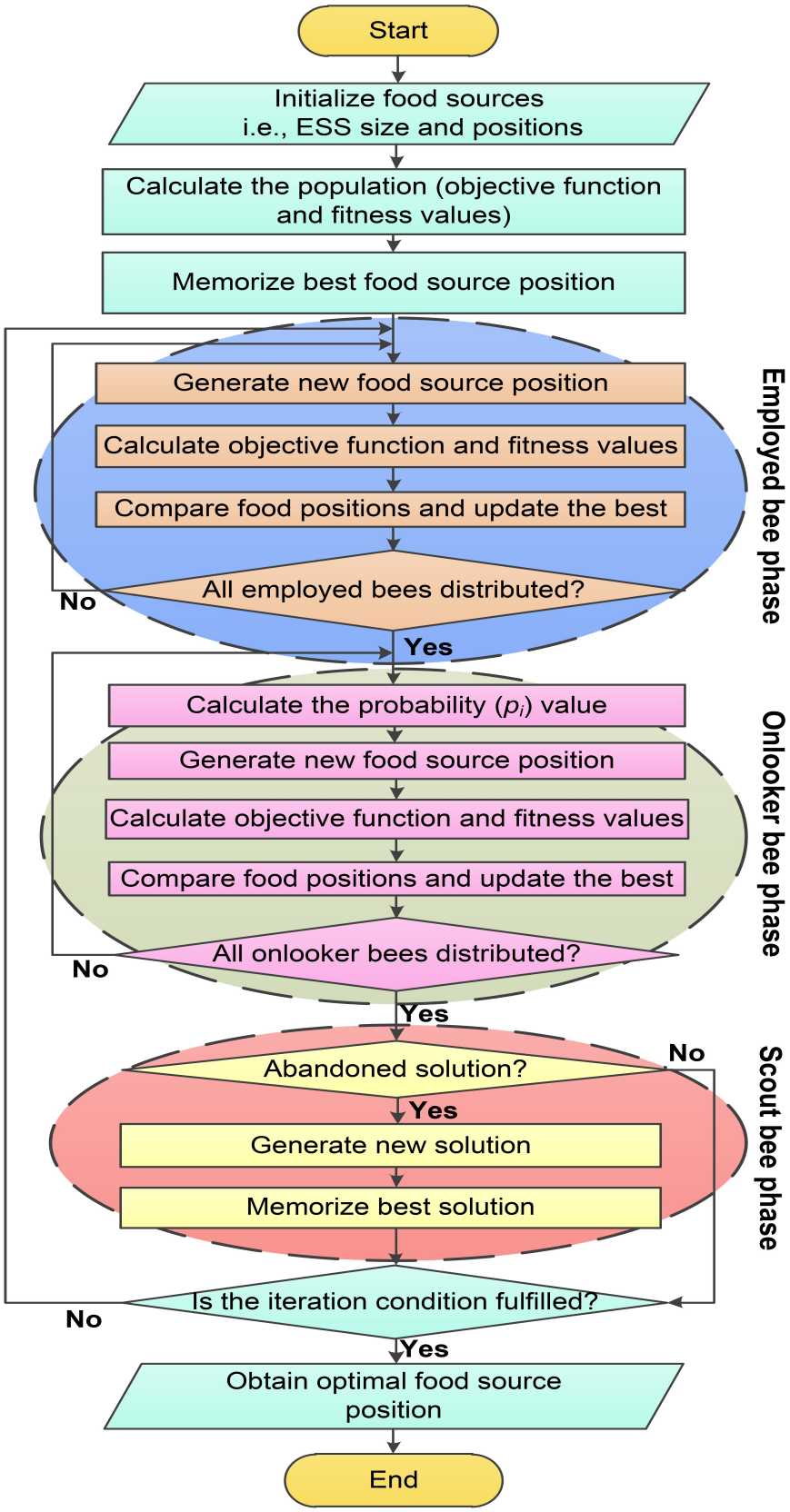

Figure 2: Flowchart of the ABC optimization approach.

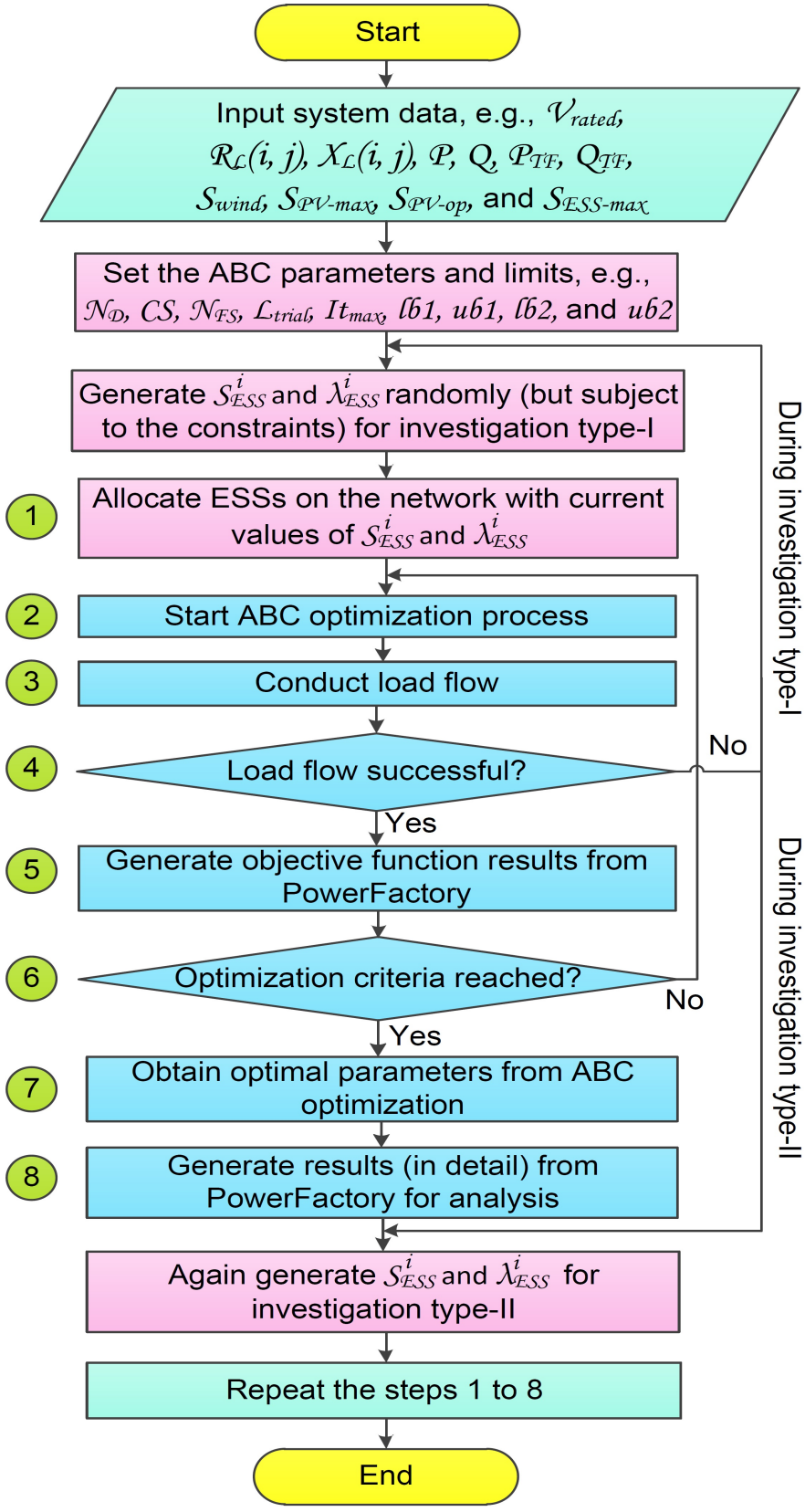

Figure 3: Flowchart of the proposed optimal distributed ESS placement approach.

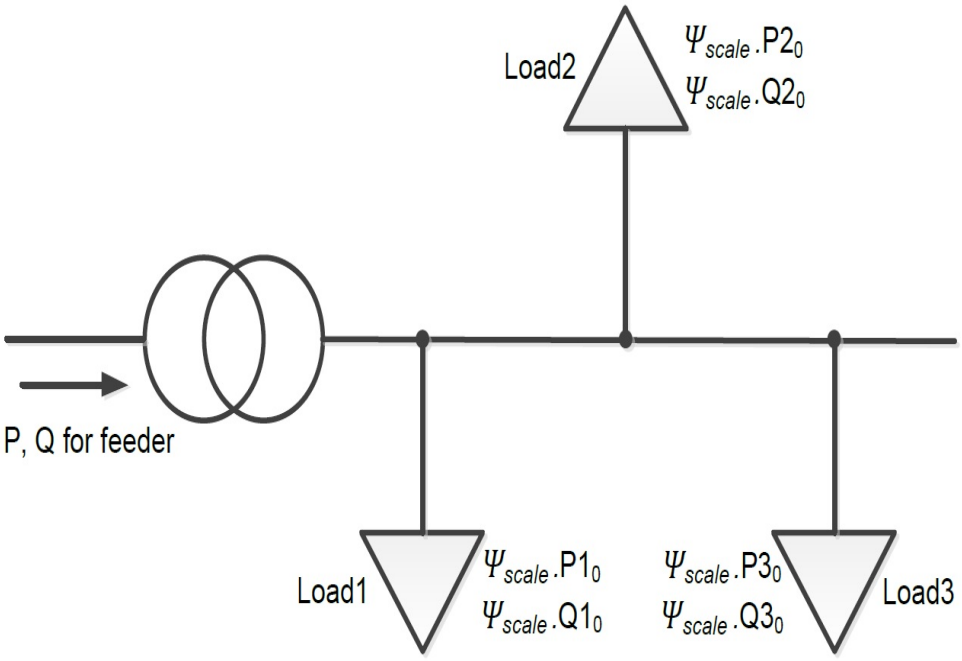

Figure 4: Load scaling of a distribution feeder [78].

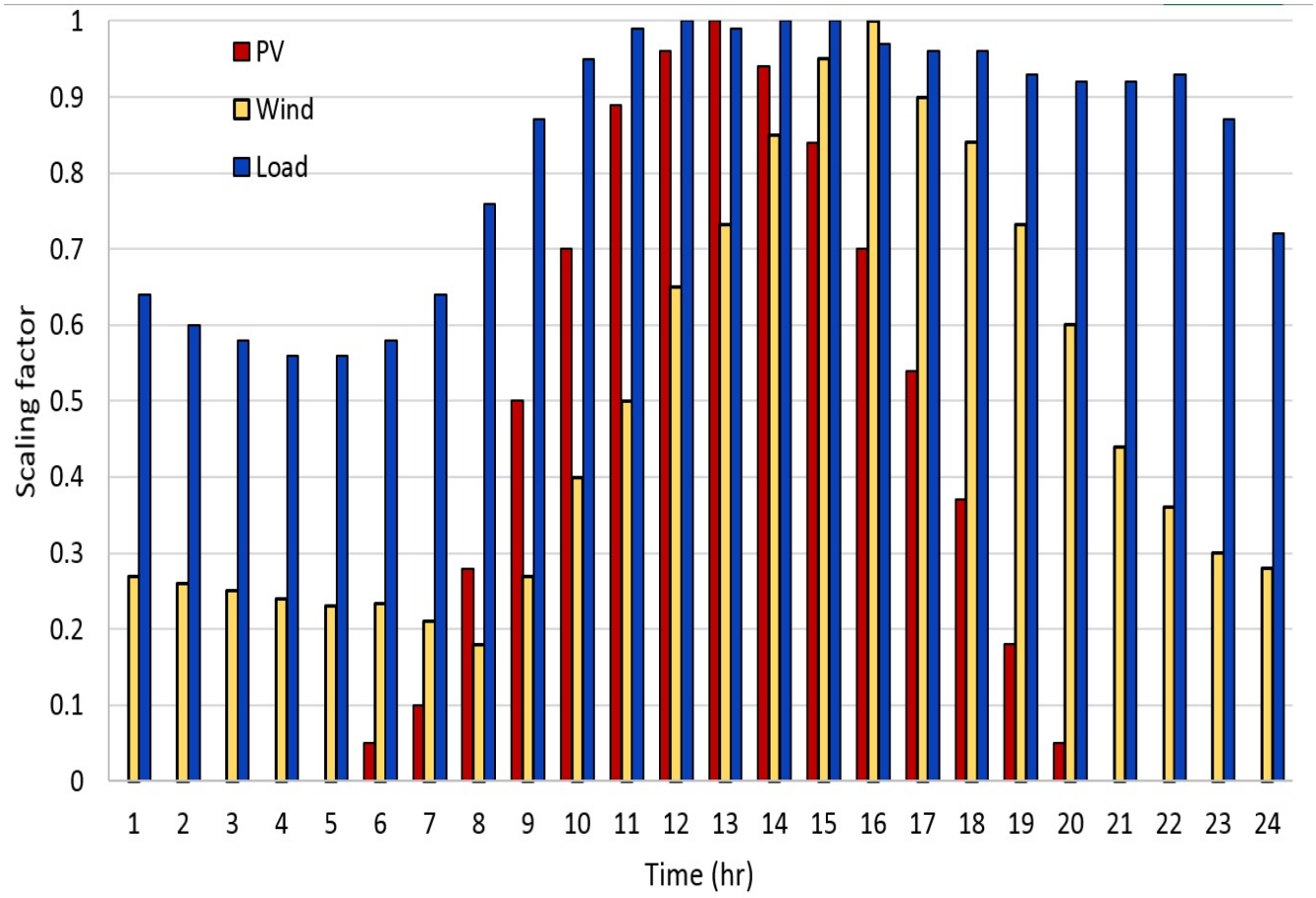

Figure 5: Time-variant scaling factors of loads and RES generation [12].

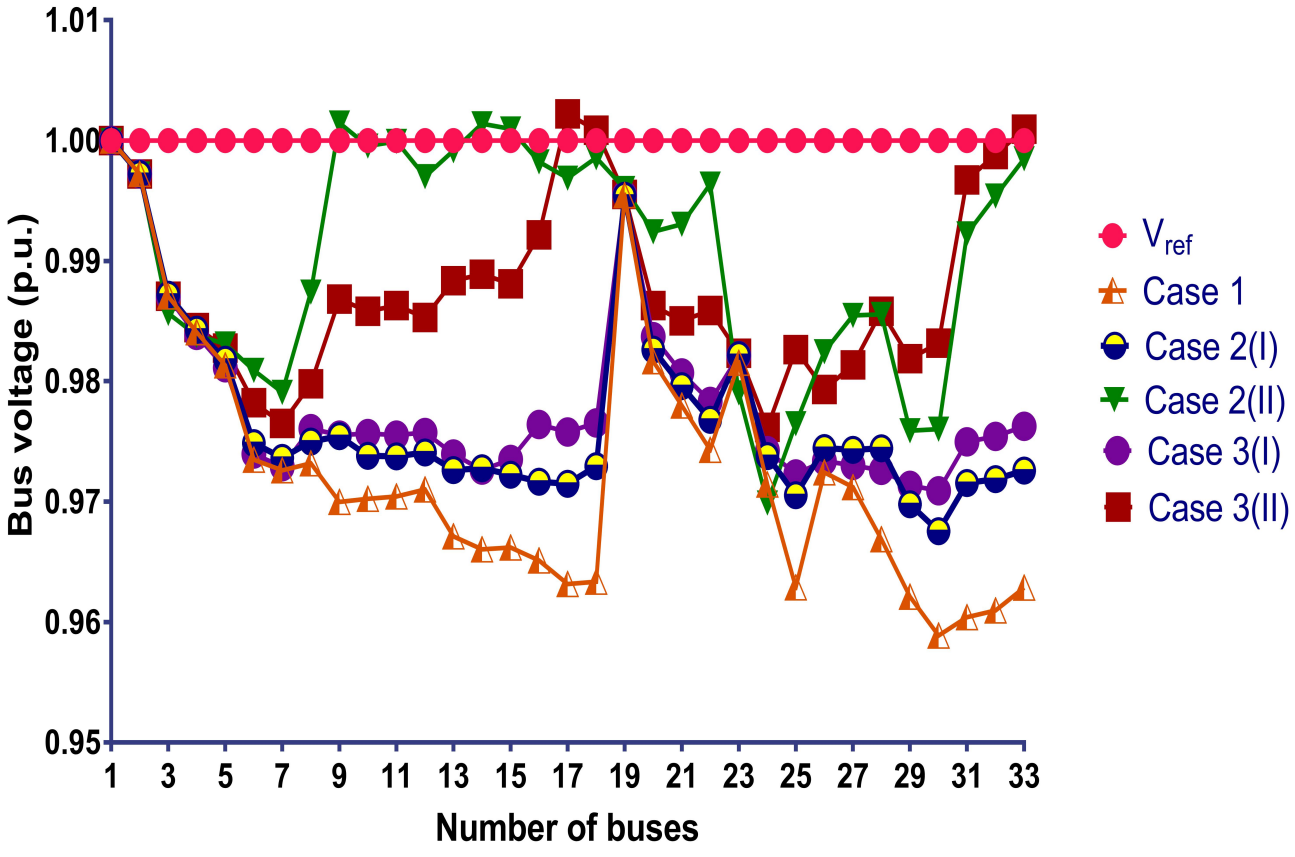

Figure 6: Voltage profiles for various cases.

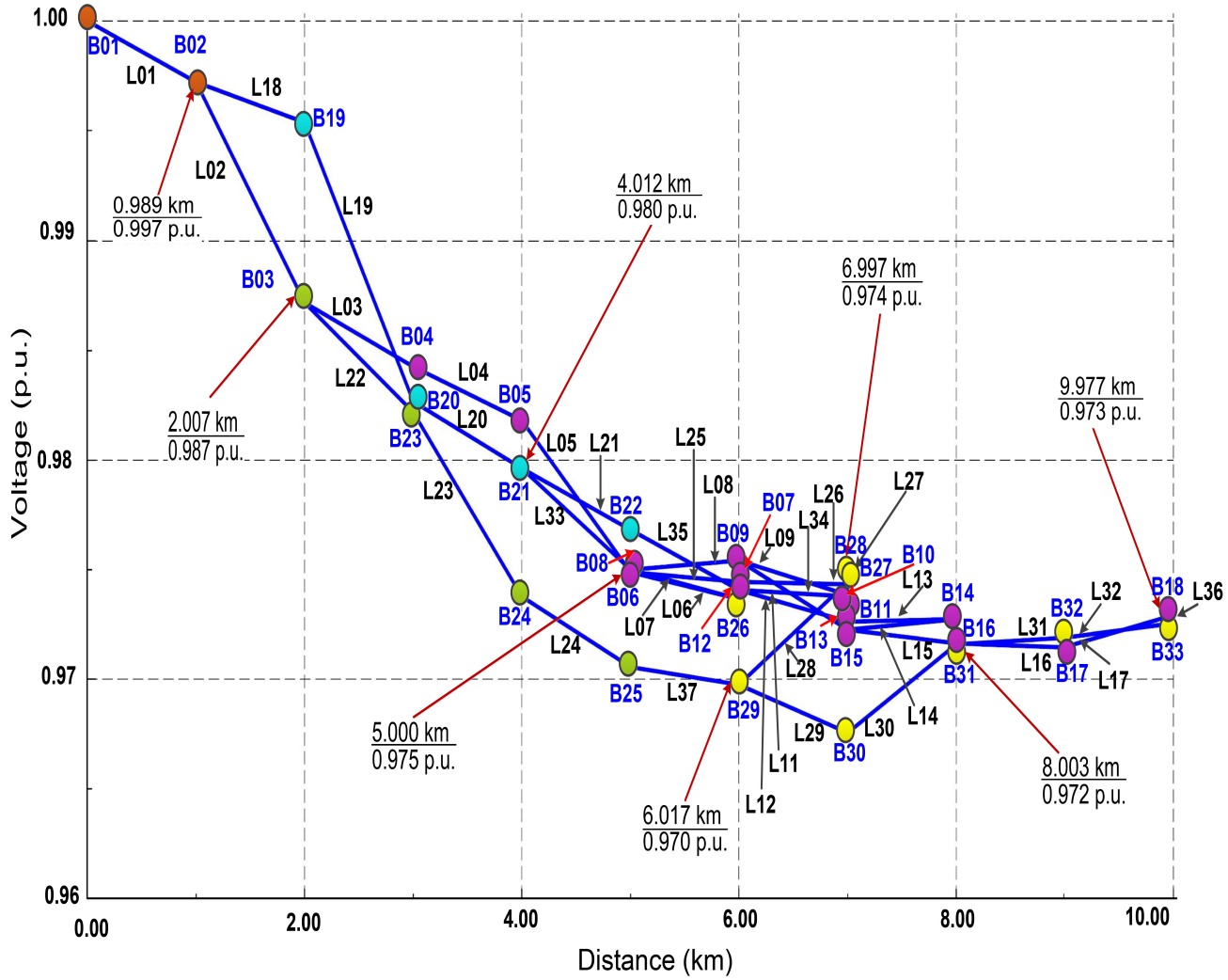

Figure 7: Voltage profile of the feeder for case 2(I).

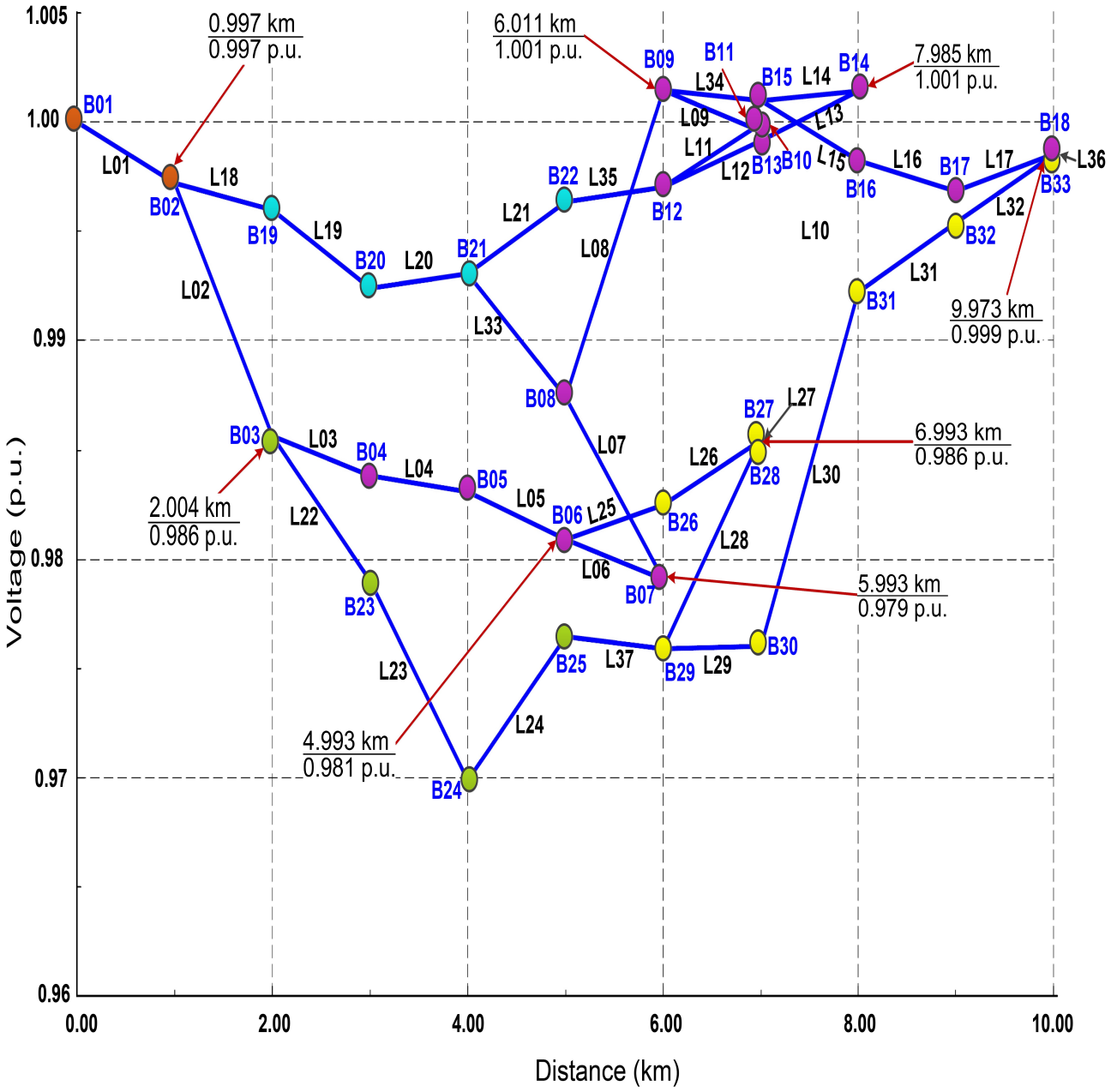

Figure 8: Voltage profile of the feeder for case 2(II).

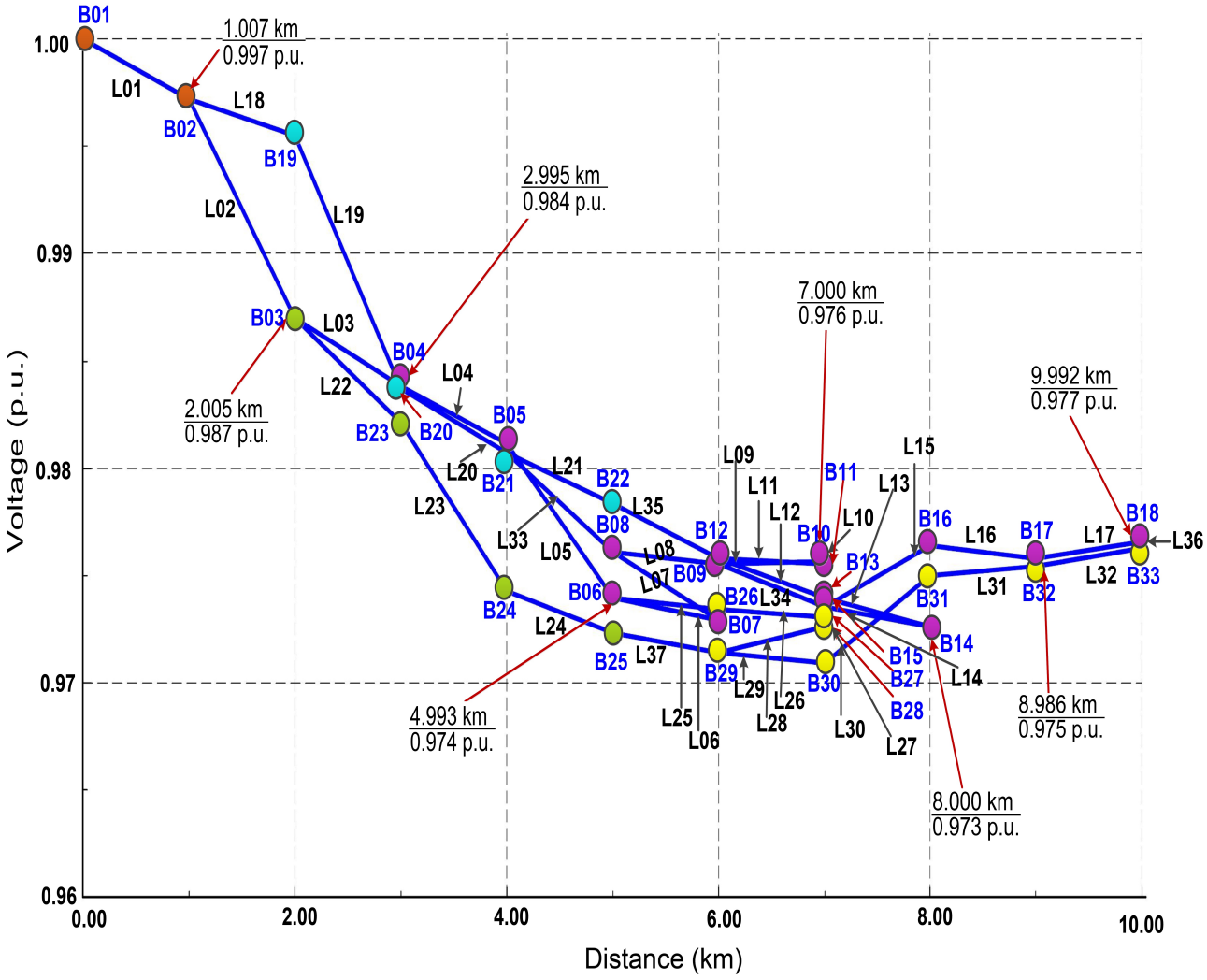

Figure 9: Voltage profile of the feeder for case 3(I).

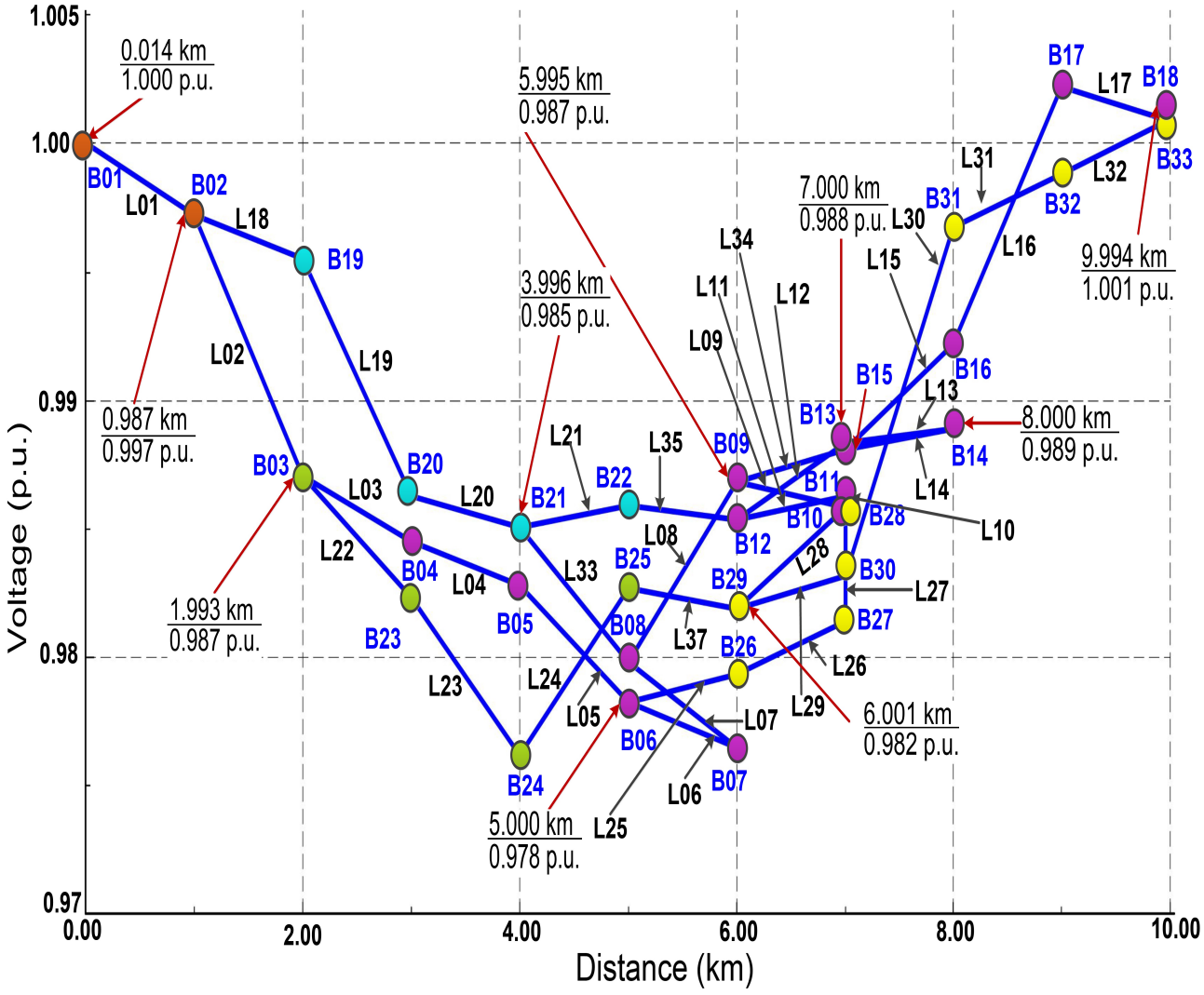

Figure 10: Voltage profile of the feeder for case 3(II).

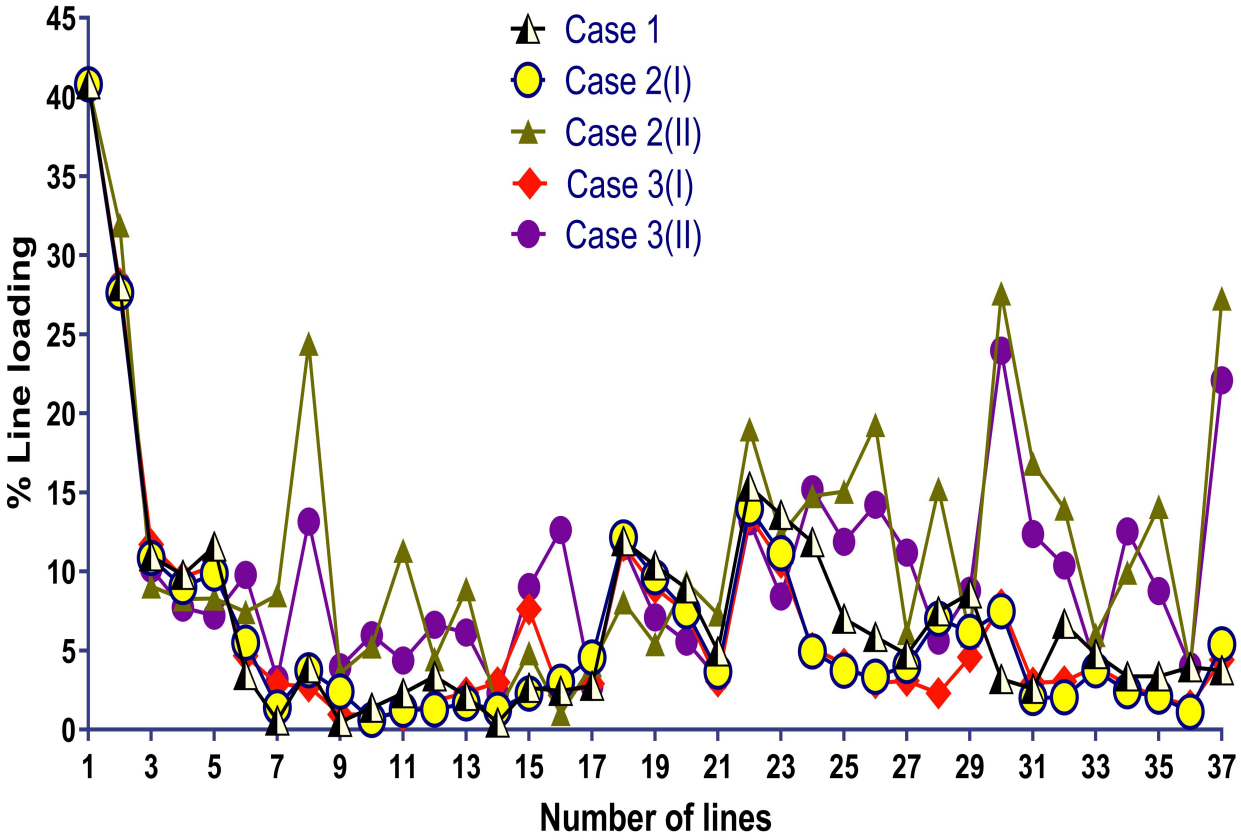

Figure 11: The percent line loading for various cases.

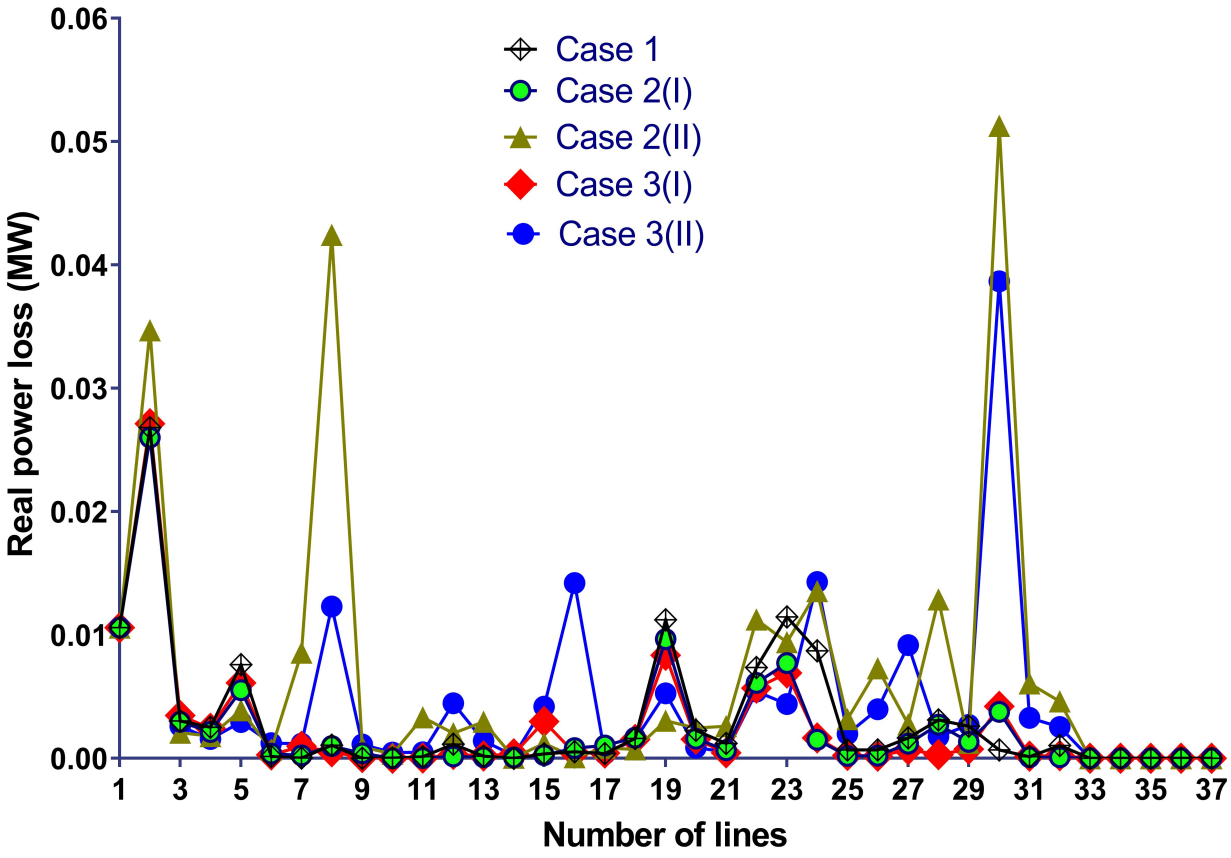

Figure 12: Real power loss for various cases.

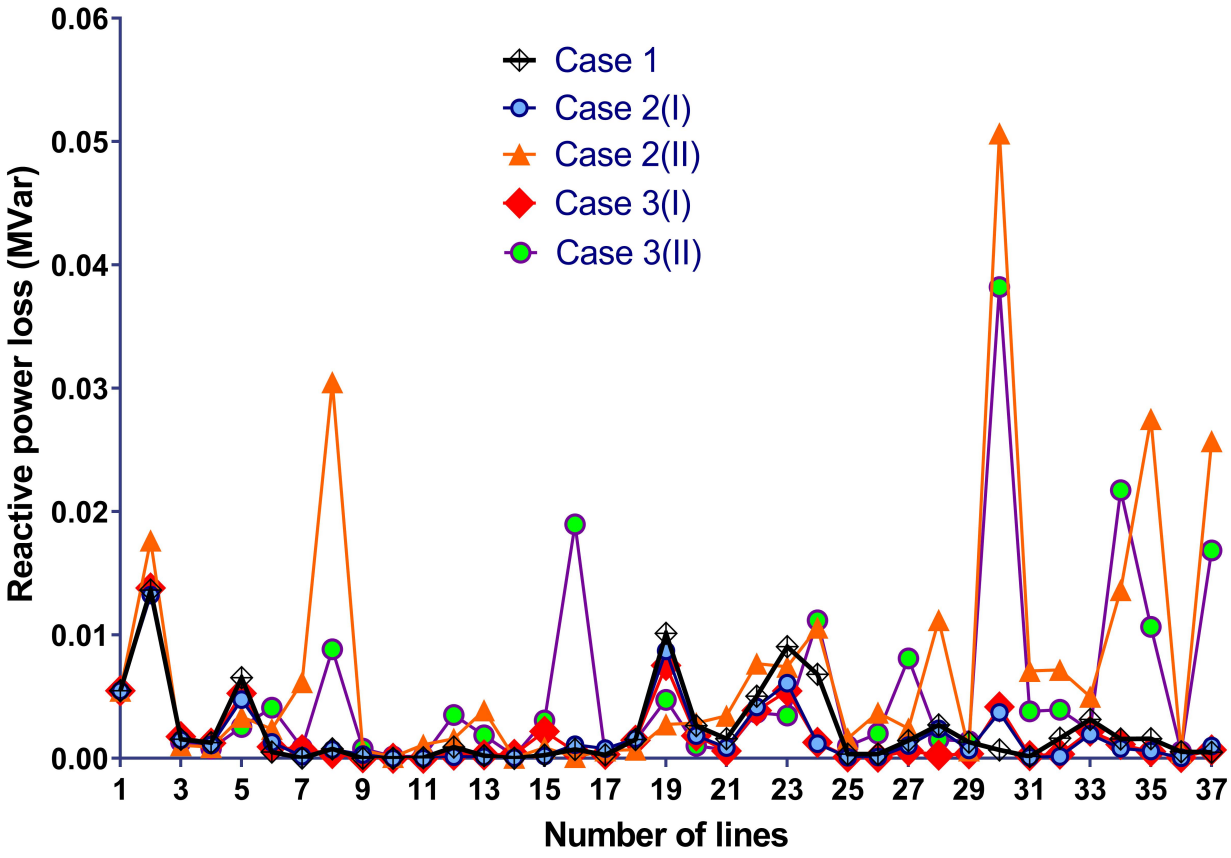

Figure 13: Reactive power loss for various cases.

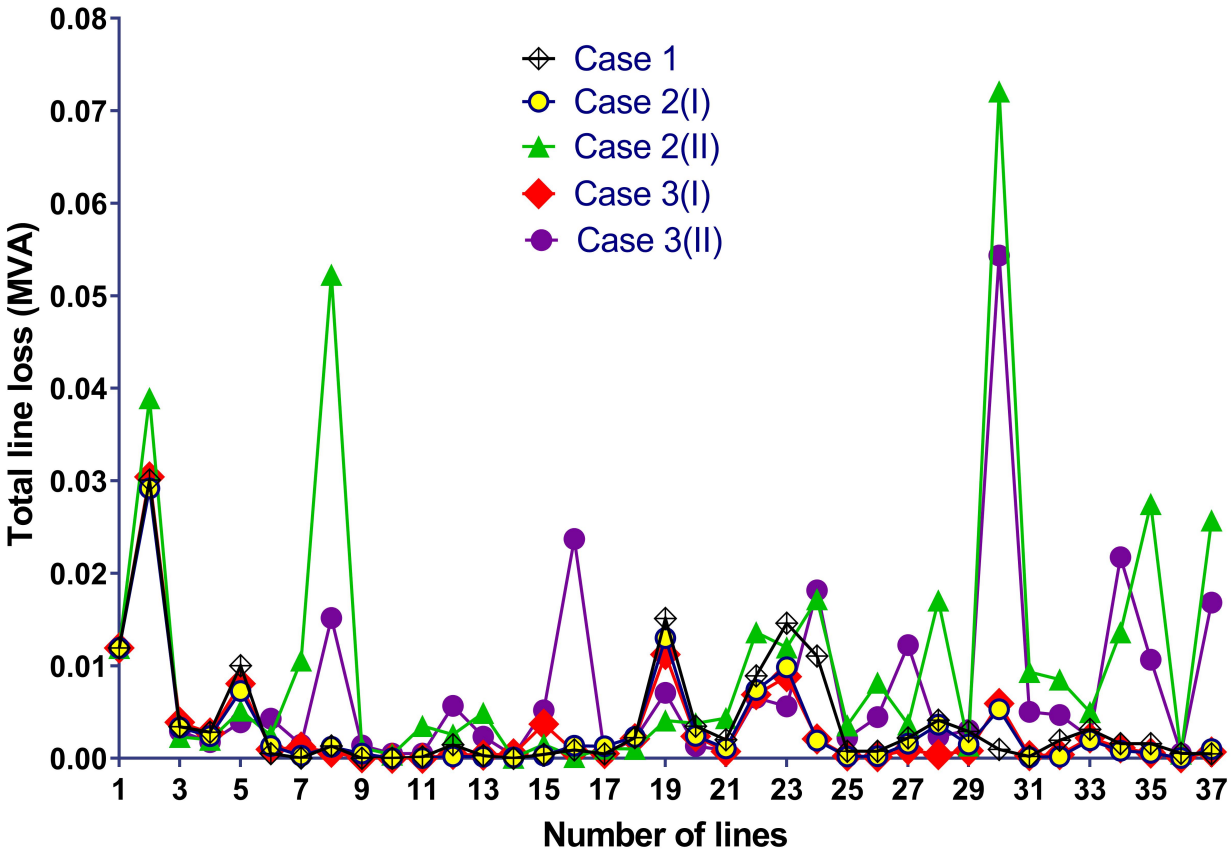

Figure 14: The total line loss for various cases.

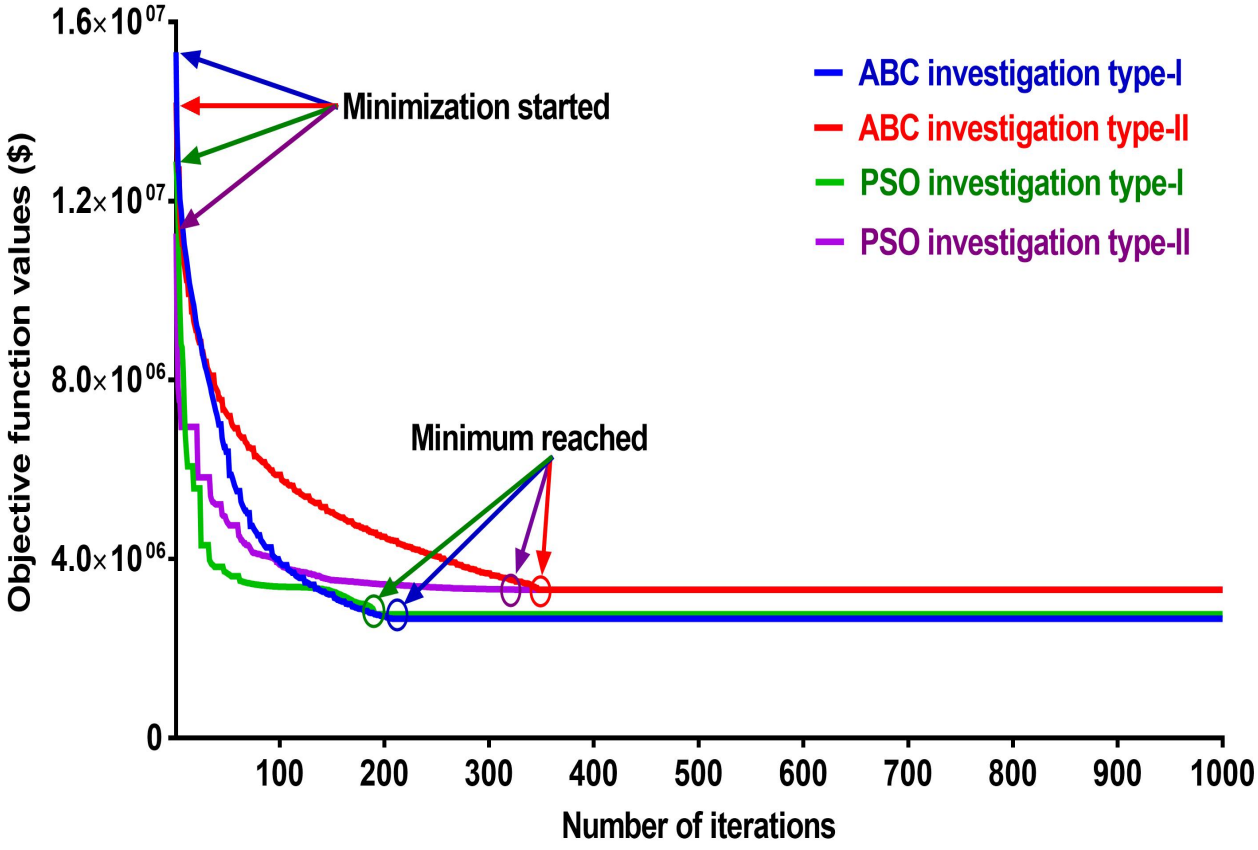

Figure 15: Convergence of ABC and PSO algorithms.

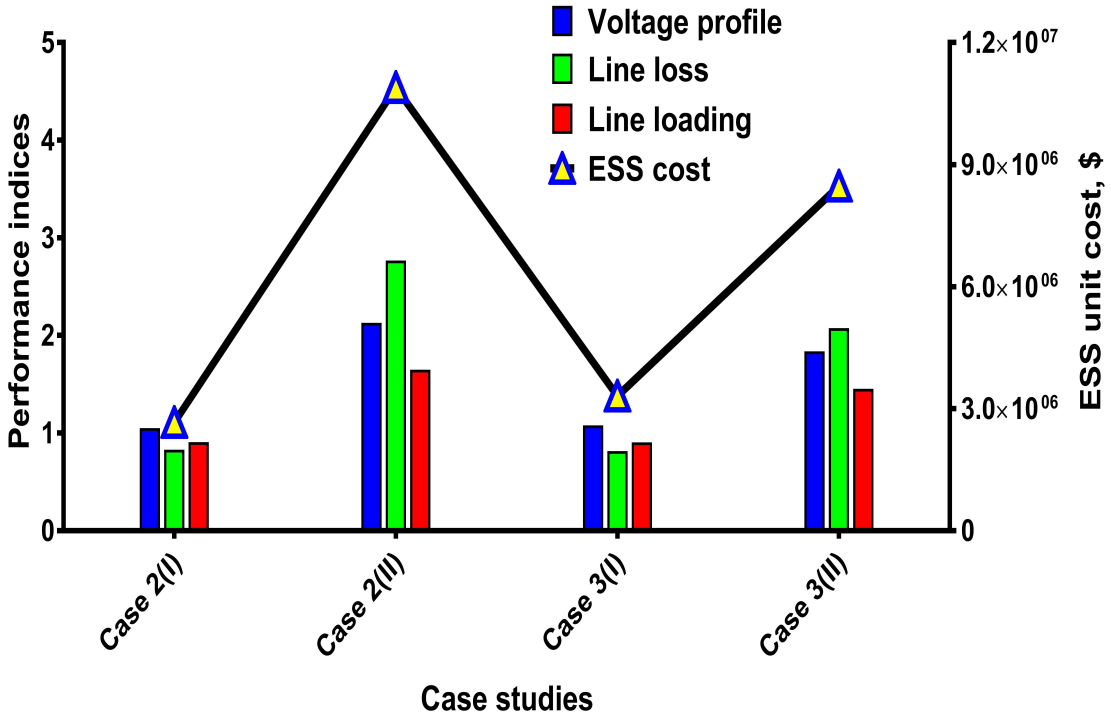

Figure 16: Performance and ESS cost comparison for various cases.

References

[1] S. van der Stelt, T. AlSkaif, W. van Sark, Techno-economic analysis of household and community energy storage for residential prosumers with smart appliances, Applied Energy 209 (2018) 266–276.

[2] A. Nemet, J. J. Klemes, N. Duic, J. Yan, Improving sustainability development in energy planning and optimisation, Applied Energy 184 (2016) 1241 – 1245.

[3] J. Yan, F. Sun, S. Choug, U. Desideri, H. Li, P. Campana, R. Xiong, Transformative innovations for a sustainable future – Part II, Applied Energy 207 (2017) 1 – 6.

[4] C. K. Das, M. A. Ehsan, M. A. Kader, M. J. Alam, G. M. Shafiullah, A practical biogas based energy neutral home system for rural communities of Bangladesh, Journal of Renewable and Sustainable Energy 8 (2) (2016) 023101.

[5] R. Moreno, R. Moreira, G. Strbac, A MILP model for optimising multi-service portfolios of distributed energy storage, Applied Energy 137 (2015) 554–566.

[6] T. A. Short, Distribution reliability and power quality, CRC Press, 2005.

[7] L. A. Schienbein, J. G. DeSteese, Distributed energy resources, power quality and reliability–background, Tech. rep., Pacific Northwest National Laboratory (2002).

[8] E. G. Carrano, F. G. Guimarães, R. H. C. Takahashi, O. M. Neto, F. Campelo, Electric distribution network expansion under load-evolution uncertainty using an immune system inspired algorithm, IEEE Transactions on Power Systems 22 (2) (2007) 851–861.

[9] C. K. Das, O. Bass, G. Kothapalli, T. S. Mahmoud, D. Habibi, Overview of energy storage systems in distribution networks: Placement, sizing, operation, and power quality, Renewable and Sustainable Energy Reviews 91 (2018) 1205 – 1230.

[10] P. Denholm, E. Ela, B. Kirby, M. Milligan, The role of energy storage with renewable electricity generation, Tech. rep., National Renewable Energy Laboratory (NREL) (2010).

[11] M. Nick, R. Cherkaoui, M. Paolone, Optimal allocation of dispersed energy storage systems in active distribution networks for energy balance and grid support, IEEE Transactions on Power Systems 29 (5) (2014) 2300–2310.

[12] N. Jayasekara, M. A. S. Masoum, P. J. Wolfs, Optimal operation of distributed energy storage systems to improve distribution network load and generation hosting capability, IEEE Transactions on Sustainable Energy 7 (1) (2016) 250–261.

[13] Y. Zhang, A. Lundblad, P. E. Campana, J. Yan, Employing battery storage to increase photovoltaic self-sufficiency in a residential building of Sweden, Energy Procedia 88 (2016) 455–461.

[14] D. Parra, S. A. Norman, G. S. Walker, M. Gillott, Optimum community energy storage for renewable energy and demand load management, Applied Energy 200 (2017) 358–369.

[15] A. Solomon, D. M. Kammen, D. Callaway, The role of large-scale energy storage design and dispatch in the power grid: A study of very high grid penetration of variable renewable resources, Applied Energy 134 (2014) 75–89.

[16] Y. Li, B. Feng, G. Li, J. Qi, D. Zhao, Y. Mu, Optimal distributed generation planning in active distribution networks considering integration of energy storage, Applied Energy 210 (2018) 1073–1081.

[17] D. Parra, M. Gillott, S. A. Norman, G. S. Walker, Optimum community energy storage system for PV energy time-shift, Applied Energy 137 (2015) 576–587.

[18] X. Li, P. E. Campana, H. Li, J. Yan, K. Zhu, Energy storage systems for refrigerated warehouses, Energy Procedia 143 (2017) 94–99.

[19] Y. Zhang, A. Lundblad, P. E. Campana, F. Benavente, J. Yan, Battery sizing and rule-based operation of grid-connected photovoltaic-battery system: A case study in Sweden, Energy Conversion and Management 133 (2017) 249–263.

[20] K. Zhu, X. Li, P. E. Campana, H. Li, J. Yan, Techno-economic feasibility of integrating energy storage systems in refrigerated warehouses, Applied Energy 216 (2018) 348–357.

[21] D. Parra, S. A. Norman, G. S. Walker, M. Gillott, Optimum community energy storage system for demand load shifting, Applied Energy 174 (2016) 130–143.

[22] A. Marini, M. A. Latify, M. S. Ghazizadeh, A. Salemnia, Long-term chronological load modeling in power system studies with energy storage systems, Applied Energy 156 (2015) 436–448.

[23] Y. Zhang, P. E. Campana, A. Lundblad, J. Yan, Comparative study of hydrogen storage and battery storage in grid connected photovoltaic system: Storage sizing and rule-based operation, Applied Energy 201 (2017) 397–411.

[24] S. Wen, H. Lan, Q. Fu, C. Y. David, L. Zhang, Economic allocation for energy storage system considering wind power distribution, IEEE Transactions on Power Systems 30 (2) (2015) 644–652.

[25] M. Nick, R. Cherkaoui, M. Paolone, Optimal siting and sizing of distributed energy storage systems via alternating direction method of multipliers, International Journal of Electrical Power & Energy Systems 72 (2015) 33–39.

[26] D. Kottick, M. Blau, D. Edelstein, Battery energy storage for frequency regulation in an island power system, IEEE Transactions on Energy Conversion 8 (3) (1993) 455–459.

[27] J. Sardi, N. Mithulananthan, M. Gallagher, D. Q. Hung, Multiple community energy storage planning in distribution networks using a cost-benefit analysis, Applied Energy 190 (2017) 453–463.

[28] R. S. Go, F. D. Munoz, J.-P. Watson, Assessing the economic value of co-optimized grid-scale energy storage investments in supporting high renewable portfolio standards, Applied Energy 183 (2016) 902–913.

[29] S. F. Santos, D. Z. Fitiwi, M. R. Cruz, C. M. Cabrita, J. P. Catalão, Impacts of optimal energy storage deployment and network reconfiguration on renewable integration level in distribution systems, Applied energy 185 (2017) 44–55.

[30] A. S. A. Awad, T. H. M. EL-Fouly, M. M. A. Salama, Optimal ESS allocation for benefit maximization in distribution networks, IEEE Transactions on Smart Grid 8 (4) (2017) 1668–1678.

[31] M. Qin, K. W. Chan, C. Y. Chung, X. Luo, T. Wu, Optimal planning and operation of energy storage systems in radial networks for wind power integration with reserve support, IET Generation, Transmission & Distribution 10 (8) (2016) 2019–2025.

[32] A. Ogunjuyigbe, T. Ayodele, O. Akinola, Optimal allocation and sizing of PV/Wind/Split-diesel/Battery hybrid energy system for minimizing life cycle cost, carbon emission and dump energy of remote residential building, Applied Energy 171 (2016) 153–171.

[33] F. J. De Sisternes, J. D. Jenkins, A. Botterud, The value of energy storage in decarbonizing the electricity sector, Applied Energy 175 (2016) 368–379.

[34] Y. Lin, J. X. Johnson, J. L. Mathieu, Emissions impacts of using energy storage for power system reserves, Applied Energy 168 (2016) 444–456.

[35] A. S. Sidhu, M. G. Pollitt, K. L. Anaya, A social cost benefit analysis of grid-scale electrical energy storage projects: A case study, Applied Energy 212 (2018) 881 – 894.

[36] A. S. A. Awad, T. H. M. El-Fouly, M. M. A. Salama, Optimal ESS allocation and load shedding for improving distribution system reliability, IEEE Transactions on Smart Grid 5 (5) (2014) 2339–2349.

[37] J. Xiao, Z. Zhang, L. Bai, H. Liang, Determination of the optimal installation site and capacity of battery energy storage system in distribution network integrated with distributed generation, IET Generation, Transmission & Distribution 10 (3) (2016) 601–607.

[38] K. Mahani, F. Farzan, M. A. Jafari, Network-aware approach for energy storage planning and control in the network with high penetration of renewables, Applied Energy 195 (2017) 974–990.

[39] A. Crossland, D. Jones, N. Wade, Planning the location and rating of distributed energy storage in LV networks using a genetic algorithm with simulated annealing, International Journal of Electrical Power & Energy Systems 59 (2014) 103–110.

[40] J. Sardi, N. Mithulananthan, D. Q. Hung, Strategic allocation of community energy storage in a residential system with rooftop PV units, Applied Energy 206 (2017) 159–171.

[41] L. Bai, T. Jiang, F. Li, H. Chen, X. Li, Distributed energy storage planning in soft open point based active distribution networks incorporating network reconfiguration and DG reactive power capability, Applied Energy 210 (2018) 1082–1091.

[42] M. Motalleb, E. Reihani, R. Ghorbani, Optimal placement and sizing of the storage supporting transmission and distribution networks, Renewable Energy 94 (2016) 651–659.

[43] A. S. A. Awad, T. H. M. El-Fouly, M. M. A. Salama, Optimal ESS allocation for load management application, IEEE Transactions on Power Systems 30 (1) (2015) 327–336.

[44] T. Yunusov, D. Frame, W. Holderbaum, B. Potter, The impact of location and type on the performance of low-voltage network connected battery energy storage systems, Applied Energy 165 (2016) 202–213.

[45] Y. Zheng, Z. Y. Dong, F. J. Luo, K. Meng, J. Qiu, K. P. Wong, Optimal allocation of energy storage system for risk mitigation of DISCOs with high renewable penetrations, IEEE Transactions on Power Systems 29 (1) (2014) 212–220.

[46] O. Babacan, W. Torre, J. Kleissl, Siting and sizing of distributed energy storage to mitigate voltage impact by solar PV in distribution systems, Solar Energy 146 (2017) 199–208.

[47] Y. Tang, S. H. Low, Optimal placement of energy storage in distribution networks, IEEE Transactions on Smart Grid 8 (6) (2017) 3094–3103.

[48] Y. Zheng, D. J. Hill, Z. Y. Dong, Multi-agent optimal allocation of energy storage systems in distribution systems, IEEE Transactions on Sustainable Energy 8 (4) (2017) 1715–1725.

[49] A. Giannitrapani, S. Paoletti, A. Vicino, D. Zarrilli, Optimal allocation of energy storage systems for voltage control in LV distribution networks, IEEE Transactions on Smart Grid 8 (6) (2017) 2859–2870.

[50] M. Ghofrani, A. Arabali, M. Etezadi-Amoli, M. S. Fadali, A framework for optimal placement of energy storage units within a power system with high wind penetration, IEEE Transactions on Sustainable Energy 4 (2) (2013) 434–442.

[51] Y. M. Atwa, E. F. El-Saadany, Optimal allocation of ESS in distribution systems with a high penetration of wind energy, IEEE Transactions on Power Systems 25 (4) (2010) 1815–1822.

[52] Y. P. Agalgaonkar, B. C. Pal, R. A. Jabr, Distribution voltage control considering the impact of PV generation on tap changers and autonomous regulators, IEEE Transactions on Power Systems 29 (1) (2014) 182–192.

[53] D. Karaboga, B. Basturk, A powerful and efficient algorithm for numerical function optimization: Artificial bee colony (ABC) algorithm, Journal of Global Optimization 39 (3) (2007) 459–471.

[54] F. S. Abu-Mouti, M. E. El-Hawary, Optimal distributed generation allocation and sizing in distribution systems via artificial bee colony algorithm, IEEE Transactions on Power Delivery 26 (4) (2011) 2090–2101.

[55] D. Karaboga, B. Akay, A comparative study of artificial bee colony algorithm, Applied Mathematics and Computation 214 (1) (2009) 108–132.

[56] D. Karaboga, B. Basturk, On the performance of artificial bee colony (ABC) algorithm, Applied Soft Computing 8 (1) (2008) 687–697.

[57] F. Gonzalez-Longatt, J. L. Rueda, PowerFactory applications for power system analysis, Springer, 2014.

[58] M. Daghi, M. Sedghi, A. Ahmadian, M. Aliakbar-Golkar, Factor analysis based optimal storage planning in active distribution network considering different battery technologies, Applied Energy 183 (2016) 456–469.

[59] T. Das, V. Krishnan, J. D. McCalley, Assessing the benefits and economics of bulk energy storage technologies in the power grid, Applied Energy 139 (2015) 104–118.

[60] X. Luo, J. Wang, M. Dooner, J. Clarke, Overview of current development in electrical energy storage technologies and the application potential in power system operation, Applied Energy 137 (2015) 511–536.

[61] M. Aneke, M. Wang, Energy storage technologies and real life applications–A state of the art review, Applied Energy 179 (2016) 350–377.

[62] K. Cavanagh, J. K. Ward, S. Behrens, A. Bhatt, E. L. Ratnam, E. Oliver, J. K. Hayward, Electrical energy storage: Technology overview and applications, CSIRO, Australia. (EP154168) (2015).

[63] T. D. Hund, N. H. Clark, W. E. Baca, Ultrabattery test results for utility cycling applications., Tech. rep., Sandia National Laboratories (SNL-NM), Albuquerque, NM (United States) (2008).

[64] E. Rodrigues, R. Godina, J. Catalo, Modelling electrochemical energy storage devices in insular power network applications supported on real data, Applied Energy 188 (2017) 315 – 329.

[65] B. Bahmani-Firouzi, R. Azizipanah-Abarghooee, Optimal sizing of battery energy storage for micro-grid operation management using a new improved bat algorithm, International Journal of Electrical Power & Energy Systems 56 (2014) 42–54.

[66] R. A. Jabr, I. Džafić, B. C. Pal, Robust optimization of storage investment on transmission networks, IEEE Transactions on Power Systems 30 (1) (2015) 531–539.

[67] B. Venkatesh, R. Ranjan, H. B. Gooi, Optimal reconfiguration of radial distribution systems to maximize loadability, IEEE Transactions on Power Systems 19 (1) (2004) 260–266.

[68] Y. Wang, N. Zhang, Q. Chen, J. Yang, C. Kang, J. Huang, Dependent discrete convolution based probabilistic load flow for the active distribution system, IEEE Transactions on Sustainable Energy 8 (3) (2017) 1000–1009.

[69] S. Devi, M. Geethanjali, Optimal location and sizing determination of Distributed Generation and DSTATCOM using Particle Swarm Optimization algorithm, International Journal of Electrical Power & Energy Systems 62 (2014) 562–570.

[70] N. Zagoras, Battery energy storage system (BESS): A cost/benefit analysis for a PV power station. Clemson University Restoration Institute, SC; September 2014. [online]. available: https://www.nrel.gov/grid/assets/pdfs/second˙grid˙sim˙zagoras.pdf. [accessed 17 october 2017].

[71] 2017-18 Synergy electricity price increases. synergy, australia. [Online]. Available: https://www.infiniteenergy.com.au/2017-18-synergy-electricity-price-increases/. [accessed 17 october 2017].

[72] D. Rastler, Electricity energy storage technology options–A white paper primer on applications, costs, and benefits, Tech. rep., Electric Power Research Institute (December 2010).

[73] F. Ren, M. Zhang, D. Sutanto, A multi-agent solution to distribution system management by considering distributed generators, IEEE Transactions on Power Systems 28 (2) (2013) 1442–1451.

[74] "State of the infrastructure report-Section 6.5.1". Western Power, Australia. [Online]. Available: https://westernpower.com.au/media/1853/state-of-the-infrastructure-report-2015.pdf. [accessed 16 june 2018].

[75] D. Karaboga, An idea based on honey bee swarm for numerical optimization, Tech. rep., Technical report-tr06, Erciyes University, Engineering Faculty, Computer Engineering Department (2005).

[76] L. dos Santos Coelho, P. Alotto, Gaussian artificial bee colony algorithm approach applied to Loney's solenoid benchmark problem, IEEE Transactions on Magnetics 47 (5) (2011) 1326–1329.

[77] Typical power output of a 5 kW solar system. Solar Choice, Australia. [Online]. Available: https://www.solarchoice.net.au/blog/5kw-solar-system-price-output-return/. [accessed 15 september 2017].

[78] DIgSILENT PowerFactory Manual, General Load, Technical Reference Documentation, DIgSILENT GmbH, Germany,, 1st Edition (2016).

[79] D. Singh, D. Singh, K. S. Verma, Multiobjective optimization for DG planning with load models, IEEE Transactions on Power Systems 24 (1) (2009) 427–436.

[80] P. Chiradeja, R. Ramakumar, An approach to quantify the technical benefits of distributed generation, IEEE Transactions on Energy Conversion 19 (4) (2004) 764–773.

[81] S. Ikeda, R. Ooka, Metaheuristic optimization methods for a comprehensive operating schedule of battery, thermal energy storage, and heat source in a building energy system, Applied Energy 151 (2015) 192 – 205.